

Diacylglycerol acyltransferase 2 links glucose utilization to fatty acid oxidation in the brown adipocytes^S

Zehra Irshad, Federica Dimitri, Mark Christian, and Victor A. Zammit¹

Translational and Experimental Medicine, Division of Biomedical Sciences, Warwick Medical School, CV4 7AL, United Kingdom

Abstract Brown adipose tissue uptake of glucose and fatty acids is very high during nonshivering thermogenesis. Adrenergic stimulation markedly increases glucose uptake, de novo lipogenesis, and FA oxidation simultaneously. The mechanism that enables this concerted response has hitherto been unknown. Here, we find that in primary brown adipocytes and brown adipocyte-derived cell line (IMBAT-1), acute inhibition and longer-term knockdown of DGAT2 links the increased de novo synthesis of fatty acids from glucose to a pool of TAG that is simultaneously hydrolyzed, providing FA for mitochondrial oxidation. DGAT1 does not contribute to this pathway, but uses exogenous FA and glycerol to synthesize a functionally distinct pool of TAG to which DGAT2 also contributes. The DGAT2-dependent channelling of ¹⁴C from glucose into TAG and CO₂ was reproduced in β3-agonist-stimulated primary brown adipocytes. Knockdown of DGAT2 in IMBAT-1 affected the mRNA levels of UCP1 and genes important in FA activation and esterification. Therefore, in β3-agonist activated brown adipocytes, DGAT2 specifically enables channelling of de novo synthesized FA into a rapidly mobilized pool of TAG, which is simultaneously hydrolyzed to provide substrates for mitochondrial fatty acid oxidation.—Irshad, Z., F. Dimitri, M. Christian, and V. A. Zammit. **Diacylglycerol acyltransferase 2 links glucose utilization to fatty acid oxidation in the brown adipocytes.** *J. Lipid Res.* 2017. 58: 15–30.

Supplementary key words adipocytes • DGAT • fatty acid/metabolism • lipolysis • adipose tissue • thermogenesis • de novo lipogenesis • β3-agonist • substrate channelling • brown adipose tissue

The diacylglycerol acyltransferases, DGAT1 and DGAT2, catalyze the last, dedicated step of triacylglycerol (TAG) synthesis. Although they catalyze the same reaction (with minor differences in substrate preferences) and are coexpressed in all the cell types in which they occur, they are functionally nonredundant. In particular, in the liver, DGAT2 is specialized for the formation of TAG from de novo synthesized fatty acids and newly formed diglycerides (DGs) thus acting upstream of DGAT1 in the de novo synthesis

of TAG (1). This renders DGAT2 essentially rate-limiting for the de novo formation of TAG in the liver (2), and is consistent with the observation that the liver of mice lacking a key enzyme of the glycerol-3-P pathway (*Gpat*^{1-/-}) is depleted of TAG and is unable to esterify de novo synthesized FA to TAG (3). Although DGAT2 also participates in the maintenance of the TAG pool(s) in lipid droplets through the lipolysis-reesterification cycling that occurs between TAG and DG (4), the esterification between preformed FA and partial glycerides is primarily performed by DGAT1 in HepG2 cells (1) and in murine liver (5). This is consistent with the observations that *Dgat*^{1-/-} and *Dgat*^{2-/-} mice have very different phenotypes, with *Dgat*^{1-/-} animals having a metabolically favorable phenotype (including lower plasma and tissue TAG) (6), whereas *Dgat*^{2-/-} animals die within several hours after birth and are devoid of TAG (lipopenic) (7). This specialization of hepatic DGAT2 for the utilization of de novo synthesized FAs is readily rationalized in view of the role of the liver in integrating glycemia, triglyceridemia, and hepatic TAG content, and accommodating large fluxes of glucose metabolism, de novo lipogenesis (DNL), and TAG synthesis and secretion (2). However, the wider applicability of this functional specialization of DGAT2 to other tissues and conditions remains to be determined (8, 9).

Brown adipose tissue (BAT) is another tissue that, like the liver, clears large amounts of both glucose and FAs (either nonesterified or as products of lipoprotein lipase action on triglyceride-rich lipoproteins) from the circulation (10). The very high rates of uptake have been suggested to

Abbreviations: ACSL, long-chain acyl-CoA synthase; ASM, acid-soluble metabolite; ATGL, adipose triglyceride lipase; BAT, brown adipose tissue; CL, CL316324; DG, diglyceride; DGAT1-iB, diacylglycerol acyltransferase 1-specific inhibitor (cis-4-[3-fluoro-4-[(5-[(4-fluorophenyl)amino]-1,3,4-oxadiazol-2-yl)] carbonyl]-amino]phenoxy) cyclohexane carboxylic acid); DGAT2-iC, DGAT2-selective inhibitor (N-(4,5-dihydro-1,2,4-thiazol-2-yl)-2-(3,4-dimethoxyphenyl)acetamide); DGAT2-iJ, 3-bromo-4-[2-fluoro-4-[(4-oxo-2-[(2-pyridin-2-ylethyl)amino] 1,3-thiazol-5(4H)-ylidene)methyl]phenoxy] benzonitrile; DNL, de novo lipogenesis; TAG, triacylglycerol; THL, tetrahydrolipstatin TOFA, 5-(tetradecyloxy)-2-furoic acid.

¹To whom correspondence should be addressed

e-mail: v.a.zammit@warwick.ac.uk

^SThe online version of this article (available at <http://www.jlr.org>) contains a supplement.

This work was supported by a Medical Research Council UK grant to V.A.Z.

Manuscript received 5 April 2016 and in revised form 18 October 2016.

Published, JLR Papers in Press, November 11, 2016

DOI 10.1194/jlr.M068197

Copyright © 2017 by the American Society for Biochemistry and Molecular Biology, Inc.

This article is available online at <http://www.jlr.org>

play a role in the regulation of glycemia and triglyceridemia, respectively (11–13). During cold exposure, BAT has the highest rate of glucose uptake and lipogenesis when compared with white adipose tissue and the liver (14). BAT glucose metabolism is independent of insulin but, during β -adrenergic stimulation, is stimulated by an increase in GLUT1 expression (via cAMP) and translocation to the plasma membrane, mediated through mTORC2 (15, 16). Although glucose makes a relatively minor direct contribution (<20%) toward thermogenesis (through glycolysis and oxidation of pyruvate) (17, 18), the contribution through oxidation of FA synthesized de novo from glucose and other lipogenic substrates [e.g., lactate (19)] could be considerably larger (13). Indeed, when nonshivering thermogenesis is maximally stimulated, BAT can account for 33% of whole-body lipogenesis, and newly synthesized FAs make a significant contribution toward the thermogenic capacity of BAT in adult rodents (14). The very substantial lipogenic capacity of BAT (20) and its activation in vivo upon cold-exposure of animals (21, 22) are accompanied by increased nuclear expression of SREBP1 and elevated gene expression of lipogenic and FA-elongation enzymes when mice are maintained at subthermoneutral temperatures (23).

Therefore, in view of the very high lipogenic potential of BAT (10, 24, 25), the contribution of de novo synthesized FA toward BAT thermogenesis may be substantial (13, 26). FAs, whether provided exogenously or synthesized de novo from glucose, activate UCPI (by overriding the inhibitory action of purine nucleotides on the protein) and provide the ultimate substrate for uncoupled respiration in brown adipocytes (27). Glucose is also required to form glycerol-3-P for the (re)synthesis of TAG from FA. Therefore, like the liver, BAT has to integrate large fluxes of glucose and fatty acid metabolism, and may be a tissue in which the distinctive functions of DGAT1 and DGAT2 may be important in directing different FA pools toward specific pathways during adrenergic stimulation, when glucose uptake, de novo lipogenesis (DNL), and TAG lipolysis are all coordinately activated (21, 22, 28). Expression profiling of mouse tissues indicates that DGAT2 is expressed in BAT judging by the high level of its mRNA expressed in the tissue (29) and that its expression is increased (more than that of DGAT1) in BAT of cold-acclimated rodents (30). Therefore, in the present study, we investigated the roles of DGAT1 and DGAT2 in the metabolism of glucose and de novo synthesized FAs, compared with that of exogenous fatty acids in a brown adipocyte cell line (IMBAT-1) and in mouse primary brown adipocytes. We identified a specific role for DGAT2 in linking glucose uptake and DNL to the formation of TAG that acts directly as a source of FAs for oxidation, independent of the uptake and metabolism of extracellular FAs.

MATERIALS AND METHODS

Preparation and culture of primary brown adipocytes

All animal maintenance and usage was made in accordance with the requirements of the Animal Welfare and Ethical Review

Body of the University of Warwick. Black c57b16 mice were used. Primary brown adipocytes were prepared from the stromal fraction resulting from the collagenase digestion of inter-scapular BAT obtained from 4-week-old mice. The stromal fraction was suspended in DMEM10, filtered through a 40 μ m strainer, and cells plated in T25 flasks. The cells were allowed to expand until 80–90% confluent with regular replacement of media. After trypsinization and resuspension in DMEM10, 5×10^4 cells/well of a 12-well plate were then plated and allowed to reach 100% confluence. Differentiation was induced by addition of medium containing insulin (1 μ g/ml), IBMX (250 μ M), triiodothyronine, T3 (1 nM), indomethacin (30 μ M), rosiglitazone (2 μ M), and dexamethasone (0.5 μ M). After 96 h, during which the medium was replenished once, the cells were switched to maintenance medium (DMEM10) supplemented with insulin, T3, and rosiglitazone only. After a further 48 h, the cells were switched to a medium which contained the same concentrations of insulin and T3, but from which rosiglitazone was omitted. After a further 48 h, the medium was changed to DMEM10 only, and the cells were used for experimental treatments.

Generation, differentiation and culture of IMBAT-1 cells

The immortalized brown adipocyte cell line (IMBAT-1) was generated as described previously (31). Briefly, preadipocytes isolated from murine interscapular BAT were immortalized by retroviral-mediated expression of temperature-sensitive SV40 large T-antigen H-2kb-tsA58. Cells were cultured in DMEM-F12 (20 mM D glucose) supplemented with 10% FBS, 1% L-glutamine, 1% penicillin/streptomycin, Amphotericin B, and 50 μ g/ml of G418 at 33°C in 5% CO₂ and 95% air-water saturated atmosphere. Unless specified otherwise, cells were passaged and harvested after treatment with 0.25% trypsin and 0.02% EDTA. For differentiation to mature adipocytes, preadipocytes were plated onto gelatin-coated plates and cultured until confluent. Induction medium containing 7.5 mM glucose, 1 μ g/ml insulin, 250 nM dexamethasone, 0.5 mM IBMX, 1 nM triiodothyronine (T3), and 125 μ M Indomethacin was added for 48 h at 37°C. Cells were then maintained in 7.5 mM glucose medium containing 1 nM T3 and 1 μ g insulin/ml for 5 days at 37°C. Unless otherwise stated, all experiments were performed on day 7 of differentiation or after a further 72 h treatment with siRNA. The experimental incubation medium was DMEM-F12 containing 7.5 mM D-glucose, 10% FBS, 1% L-glutamine, 1% penicillin/streptomycin, 1 mM L-carnitine, 0.75 mM oleate with 0.25% BSA, and 0.75 mM glycerol.

SiRNA-mediated knockdown of DGAT1 or DGAT2

Transfections were carried out on day 7 of differentiation using Smartpool siRNA, designed by the manufacturers for DGAT1 and DGAT2, and transfection reagent lipofectamine RNAiMax, following the manufacturer's instructions. Differentiated adipocytes were dissociated with trypsin/EDTA followed by addition of DMEM/F12 with 10% FBS. Mixtures of transfection reagents, OptiMEM medium, and 10 μ M siRNA-DGAT1 or 10 μ M siRNA-DGAT2 or 10 μ M siRNA-control were incubated at room temperature for 25 min. They were then added to the dissociated cells along with antibiotic-free DMEM-F12 (7.5 mM glucose). Control cells were treated with scrambled siRNA. Media were changed after 24 h and cells were cultured for further 48 h at 37°C in maintenance medium. Preliminary experiments established that optimal knockdowns were achieved after 72 h of siRNA treatment.

Measurement of the incorporation of ¹⁴C-glucose label into CO₂ and cellular TAG

IMBAT-1 or primary brown adipocytes cells plated in gelatin-coated 6-well plates containing 7.5 mM glucose medium were incubated for 2 h in the presence or absence of the β 3-adrenergic

agonist CL (10 μ M) before the addition of label to start the measurements. Preliminary experiments established the incorporation of [U - 14 C]glucose into labeled products was linear for 2 h and this period was used routinely when [U - 14 C]glucose incorporation was studied. Where indicated, oleate or palmitate (0.75 mM plus 0.25% albumin) and glycerol (0.75 mM) were added to the incubations. When incorporation of label from 1- 14 C]oleate, U - 14 C] palmitate, or 2- 3 H]glycerol was measured, the labeling period was 1 h to ensure linearity of incorporation into TAG. In one series of experiments, labeling with exogenous 1- 14 C]oleate was extended to 8 h to monitor the release of 14 CO $_2$. When effects of DGAT1 or DGAT2 inhibition were studied, the appropriate inhibitors were added 30 min before the start of the incubations with the label. Where indicated, etomoxir (80 μ M) was added 30 min before the start of the experimental period by addition U - 14 C]-glucose label. Lipolysis was inhibited by addition of tetrahydrolip- statin (THL, 200 μ M) or Atglistatin (10 μ M) at the same time as the addition of CL; i.e., 2 h before the addition of U - 14 C]-glucose label.

Measurement of 14 CO $_2$ labeling

Formation of 14 CO $_2$ after incubation of cells with labeled substrates for the required period of time was measured by transferring 1 ml of the incubation medium to a 20 ml glass conical flask containing a 0.5 ml Fisher center well holding filter paper to which 400 μ l of benzethonium hydroxide had been added (32). The flask was stoppered and 1.0 ml of 1 M H $_2$ SO $_4$ was injected through the rubber stopper. The flasks were shaken for 60 min at 37°C to allow the liberated 14 CO $_2$ to be absorbed by the benzethonium hydroxide, after which the radioactivity associated with the contents of the center well was quantified using a liquid scintillation counter.

Measurement of incorporation of label into TAG

At the end of the incubation period, the cells were washed with cold PBS and total lipids were extracted from them using a chloroform/methanol mixture (2:1 v/v) (33). The chloroform layer was aspirated into a glass tube and dried under a stream of N $_2$ gas. The dried material was resolubilized in chloroform (500 μ l) and the entire volume was applied onto a TLC plate coated with Silica Gel 60 for separation of the radioactive triglyceride product, using hexane/diethyl ether/formic acid (70:30:1, v/v/v) as the mobile phase. A TAG-standard (tripalmitin) was used to identify the position of the TAG band visualized using iodine vapor. The radioactivity associated with each band was quantified after scraping into scintillation vials, addition of scintillant (Ultima GoldTM, Perkin Elmer) and measuring the associated radioactivity using a scintillation counter.

Saponification of the total lipids was performed as described in (34) with minor modifications. The cellular total lipid extract was dried and dissolved in 0.75 ml of 30% KOH and heated at 70°C for 10 min. An equal volume of 95% ethanol was then added and the mixture was heated at 70°C for 2 h. After cooling, the aqueous fraction was acidified with 3M HCl and extracted three times with light petroleum. The organic fraction was evaporated, redissolved in 1 ml of light petroleum, transferred to a scintillation vial, and quantified as the TAG-acyl fraction. The remaining aqueous fraction contained the TAG-glycerol fraction; a 0.5 ml aliquot of this sample was taken and measured for radioactivity using scintillation counter.

Real time PCR quantitation of mRNA expression

Total RNA was extracted from IMBAT-1 cells using TRIzol reagent. cDNA was prepared using reverse transcription. Briefly, RNA (1 μ g) was mixed with oligodT (1 μ l) in a final volume of 12 μ l by adding RNase free water. Samples were heated at 70°C

for 5 min before chilling on ice. Subsequently, 8 μ l of mixture containing RNase inhibitor (10 U/ μ l), dNTPs (10 mM), Bioscript reverse transcriptase and RNase free water were added to each sample. Samples were heated at 40°C for 60 min and the reaction was stopped by heating to 70°C for 10 min. The cDNA formed was mixed with 180 μ l of nuclease-free water and stored at -20°C. Samples were thawed only once before quantification. RT-PCR was performed using SYBR green dye and expression for all the samples ($n \geq 3$) was calculated by using the DCt method, incorporating the efficiencies of each primer. The variances of input cDNA were normalized against the levels of three housekeeping genes: L19, B-actin, and 36B4. Melting curve analysis confirmed amplification specificity. The primers used are detailed in supplemental Table S1.

Statistical analyses

Differences between means for independent groups of data were analyzed by ANOVA followed by the post hoc Tukey test.

Materials

DMEM10, DMEMF12, etomoxir sodium salt, CL, L-carnitine, benzethonium hydroxide, light petroleum (bp: 40-60°C), glyceryl tripalmitate, sodium oleate, insulin, IBMX, Indomethacin, and 3,3',5'-triiodo-L-thyamine were purchased from Sigma-Aldrich. TLC-pre-coated plates, 10 ml conical flasks with center wells, lipofectamine, and RNAiMax were purchased from Fischer Scientific. Rosiglitazone was from Cayman Chemical. Radiolabeled [U - 14 C] glucose (specific activity 250-360 mCi/mmol), [U - 14 C] Oleic acid (specific activity: 40-60 mCi/mmol) and [3 H] glycerol (specific activity 0.5-1.0 Ci/mmol) was purchased from Perkin Elmer LAS (UK). ON-TARGETplus Mouse Dgat1 smartpool siRNA, ON-TARGETplus Mouse Dgat2 smartpool siRNA, and ON-TARGETplus nontargeting siRNA were purchased from GE Healthcare UK. Of the three inhibitors of DGAT activity used, DGAT1iB (cis-4-[3-fluoro-4-[(5-[(4-fluorophenyl)amino]1,3,4-oxadiazol-2-yl)carbonyl]-amino]phenoxy) cyclohexane carboxylic acid) and DGAT2-iC (N-(4,5-dihydropnaphthol[1.2-d]thiazol-2-yl)-2-(3,4-dimethoxyphenyl)acetamide) were obtained from Astra Zeneca and have been used previously as DGAT1 and DGAT2 inhibitors, respectively (33). A third inhibitor, DGAT2-iJ (3-bromo-4-[2-fluoro-4-[(4-oxo-2-[(2-pyridin-2-ylethyl)amino]1,3-thiazol-5(4H)-ylidene)methyl]phenoxy] benzonitrile) was obtained from Janssen Research and Development UK, and has been used previously as a specific DGAT2 inhibitor (5). All primers were purchased from Sigma-Aldrich.

RESULTS

Experiments using the brown adipocyte-derived cell line IMBAT-1

In view of the large amount of preliminary work that was needed to establish the conditions under which the metabolic fluxes of interest could be measured, and the concentrations of inhibitors required, we used a well-established brown adipocyte-derived cell line, IMBAT-1. This cell line has been well characterized, and has been shown to express all the proteins that are characteristic of brown adipocytes, especially UCP1 (35). Their use also allowed us to verify the effects observed with specific DGAT1 and DGAT2 inhibitors through the efficient knockdown of the two proteins in these cells using siRNA. The main findings were validated using primary brown adipocytes (see below).

DGAT2 mRNA expression is preferentially induced during differentiation. We investigated the expression of DGATs across a panel of murine tissues. DGAT2 mRNA was most highly expressed in BAT, and present at much lower levels in white adipose tissue, liver, intestine, and mammary gland (Fig. 1). DGAT1 mRNA was most highly expressed in the intestine, followed by BAT, white adipose tissue, and mammary gland. We then studied the profile of mRNA expression for both DGATs, compared with the differentiation marker aP2 during brown adipocyte differentiation. All three mRNAs were induced at day 2 of differentiation, but whereas DGAT1 mRNA was induced moderately (7-fold) during the first days of differentiation, leveling off thereafter and declining on day 6, DGAT2 mRNA was induced 50-fold and continued to be induced throughout the period of differentiation (Fig. 2). This time course of the expression of the two genes is the opposite to that previously described during the differentiation of white adipocytes, in which an initial peak in DGAT2 expression (during initial differentiation with glucose as the main substrate) is overtaken by a sustained expression of DGAT1 mRNA during the latter stages of differentiation (35).

β3-adrenergic stimulation increases incorporation of de novo synthesized FA into TAG and CO₂. We next measured the

rates of labeling from U-¹⁴C-glucose into TAG and CO₂ in IMBAT-1 cells, and ascertained that they were linear during the 2 h period of the incubations (not shown). Stimulation of IMBAT-1 cells with the β3-agonist CL316324 (CL) for 2 h before the start of incubations (by addition of U-¹⁴C-glucose label) resulted in a significant increase in the incorporation of ¹⁴C-label from glucose into CO₂ (Fig. 3A). The rates of CL-stimulated glucose incorporation were 22.8 ± 1.3 and 50.6 ± 1.0 pmol/h/10⁶ cells for TAG-acyl and TAG-glycerol moieties, respectively. The incorporation into CO₂ was 10.6 ± 1.4 pmol/h/10⁶ cells, although this flux is not directly comparable to the previous two, as *i*) ¹⁴CO₂ is generated both during lipogenesis and FA oxidation, and *ii*) ¹⁴CO₂ derived from the oxidation of de novo synthesized FAs will have been diluted by unlabeled acyl moieties within the preexisting TAG pool. From the observation that 10⁶ cells yield ~10 mg wet weight of cellular material, it is calculated that these rates are of the same order of magnitude as the values reported for glucose uptake (~7.2 μm/h/g) and de novo lipogenesis rates (~4.8 μm/h/g) in cold-acclimated rats in vivo (14, 30).

Etomoxir [an inhibitor of CPT1 that controls FA entry into mitochondria (36)] inhibited CO₂ labeling marginally under basal conditions (Fig. 3) suggesting that, as expected, in the absence of CL-stimulated TAG lipolysis, CO₂

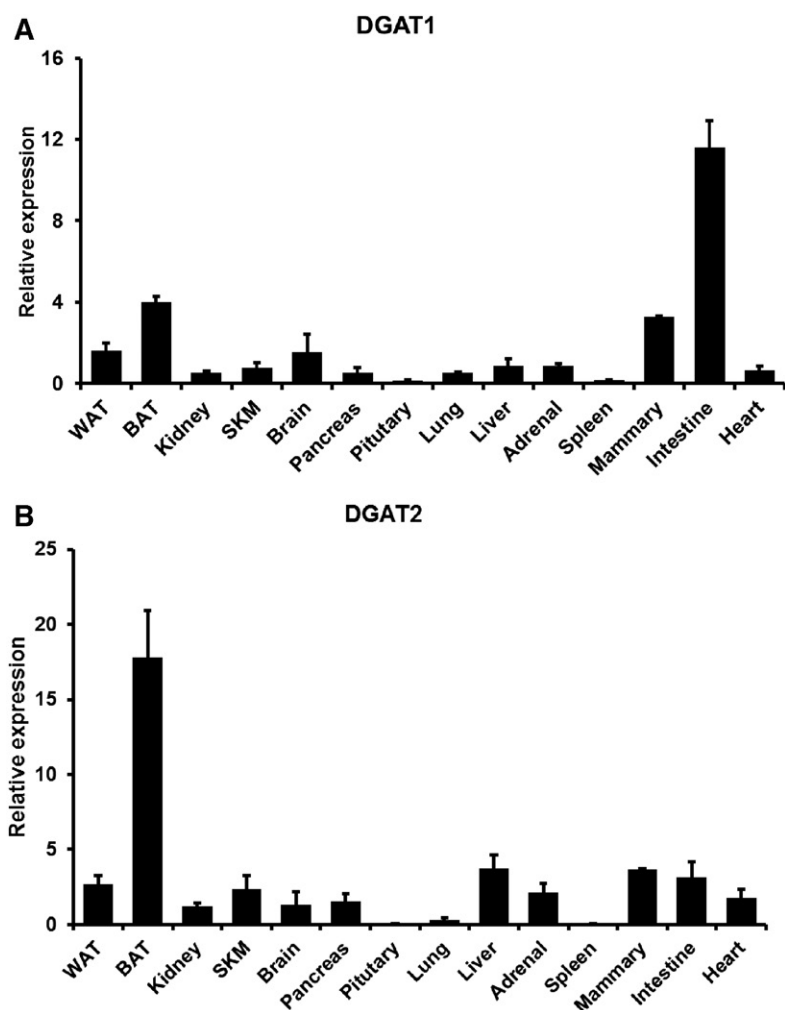


Fig. 1. DGAT1 and DGAT2 mRNA expression in mouse tissues. The levels of mRNA expression of (A) DGAT1 and (B) DGAT2 were measured in the mouse tissues indicated. Values are means (± SEM) for three separate determinations. See Methods section for details of the normalization of the data. WAT, white adipose tissue; SKM, skeletal muscle.

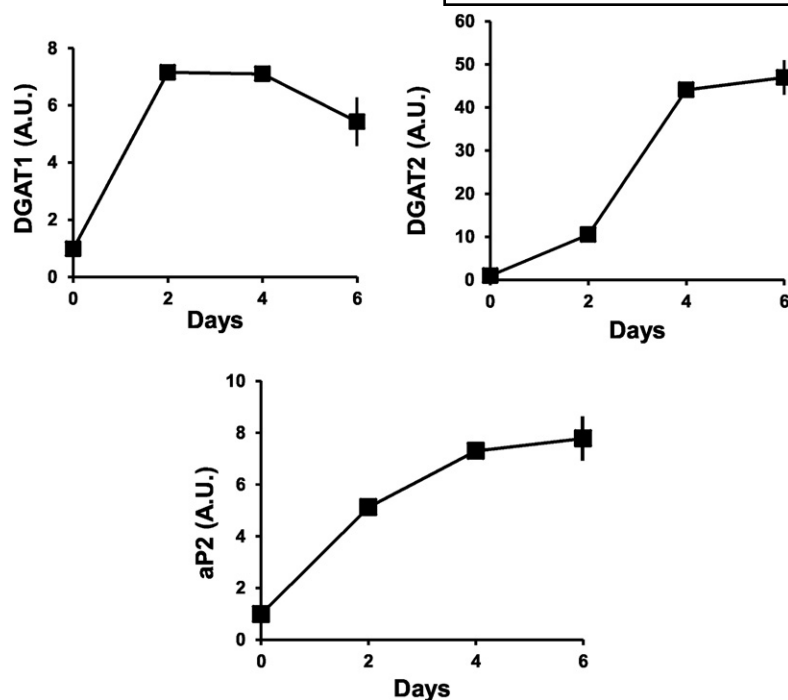


Fig. 2. Expression of DGAT1, DGAT2 and aP2 during differentiation of IMBAT-1 cells. IMBAT-1 cells were differentiated for 6 days (see Methods section). The fold-activation of DGAT1, DGAT2, and aP2 mRNA expression relative to that at day 0, during subsequent differentiation. The variances of input cDNA were normalized against the levels of three housekeeping genes: L19, B-actin, and 36B4. Values are means (\pm SEM) for three separate determinations for separate cell preparations. Note different scale of y axis for DGAT2. Where error bars are not shown, they lie within the symbols.

labeling from glucose was due mostly to that generated in the course of lipogenesis. The increase in CO_2 labeling induced by CL was totally prevented by etomoxir (Fig. 3A). As a result, it could be calculated that CL increased the rate of $^{14}\text{CO}_2$ labeling due to CPT 1-dependent oxidation of de novo synthesized FAs by ~ 4 -fold (Fig. 3A).

Stimulation of the cells with CL also activated incorporation of label from $\text{U-}^{14}\text{C}$ -glucose into both parts of the TAG molecule (glyceryl and acyl, Fig. 3B and C, respectively) although differentially. Stimulation of $\text{U-}^{14}\text{C}$ -glucose incorporation into the acyl moieties of the TAG molecule was consistently significantly higher (200%) than that into the glyceryl moiety of TAG (50%), indicating that, whereas increased glucose uptake by the cells by CL may have been a common contributor toward the increased labeling of TAG from glucose (25), de novo lipogenesis was stimulated independently of, and to a higher extent than, the pathway leading from glucose to triose phosphates (the last common intermediates of glycerol-3-P and FA formation). Etomoxir did not affect incorporation of glucose into TAG-acyl or TAG-glyceryl moieties, confirming that its action is specific to the inhibition of FA oxidation.

CL-stimulation of glucose incorporation into TAG-FA and their oxidation is ATGL-dependent. To test the possible role of TAG synthesis and hydrolysis in the provision of glucose-derived FA for oxidation, we tested the effects of inhibition of TAG hydrolysis, using Atglistatin (a specific inhibitor of adipose triglyceride lipase, ATGL) and the nonspecific lipase inhibitor THL. Both inhibitors prevented all the effects of CL treatment on CO_2 and TAG labeling from $\text{U-}^{14}\text{C}$ -glucose without affecting basal rates (Fig. 4). CL-stimulation of the incorporation of glucose into both acyl and glyceryl moieties of TAG was totally prevented by ATGL inhibition by Atglistatin. This indicated that a metabolite

generated by TAG lipolysis activates one or more steps in the pathway leading from glucose to TAG synthesis, and occurs independently of the interruption of the provision of FA for oxidation as a result of the inhibition of TAG hydrolysis. This positive feedback on TAG synthesis supports previous observations that TAG lipolysis generates signaling molecules that affect lipogenic fluxes (37–39).

Oxidation of de novo synthesized FAs is DGAT2-dependent.
INHIBITOR STUDIES. In view of the preferential activation of the esterification of de novo synthesized FA into TAG labeled from glucose, we studied the possibility that DGAT1 and DGAT2 may have different roles in the esterification of newly synthesized FA into TAG after $\beta 3$ -stimulation of IMBAT-1 cells. We used three compounds that have previously been well characterized as specific inhibitors of the two DGATs. Compound DGAT1-iB was previously used (1, 33, 40, 41) as a highly specific inhibitor of DGAT1, Compound DGAT2-iC (see Methods) was used in (1) as a selective inhibitor of DGAT2 at lower concentrations, and compound DGAT2-iJ was developed and used as a highly specific inhibitor of DGAT2 [(5); see Methods]. As these compounds have been developed as inhibitors of human enzymes, we performed dose-response studies to ascertain that they were effective inhibitors of TAG synthesis in IMBAT-1 cells at concentrations that were not deleterious to cell viability. The concentrations required for each compound to inhibit incorporation of $\text{U-}^{14}\text{C}$ -glucose into the glyceryl or acyl moieties of TAG (see supplemental Figure S1) were similar to those found to be effective in HepG2 cells and on the recombinant human enzymes (1, 5, 33). In the same experiments, we quantified cell viability, as judged by MTT mitochondrial viability assays, at the end of the 2 h incubations. Thereafter, the effects of DGAT1 or DGAT2 inhibition were investigated in detail, using single

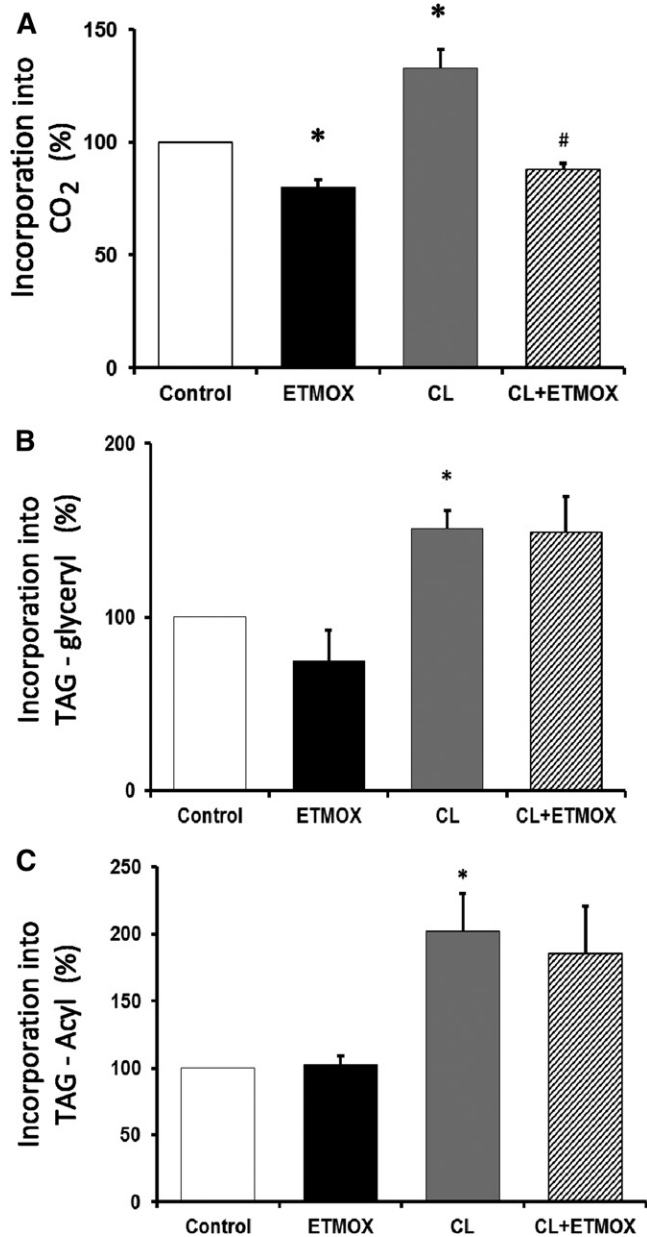


Fig. 3. Etomoxir selectively prevents the increase in glucose-derived CO₂ formation after β₃-adrenergic stimulation of IMBAT-1 cells but not the increased incorporation into the glycerol and acyl moieties of TAG. Cells were incubated with CL for 2 h, followed by a further incubation period of 2 h, at the start of which U-¹⁴C-glucose label was added (at zero time) as described in the Methods section. Incorporation of label was measured into (A) CO₂ and (B) glycerol- and (C) acyl-moieties of TAG. Etomoxir was added 30 min before the addition of label. Data are means (± SEM) for three separate experiments and are expressed with respect to paired controls, which are set at 100% for each experiment. Values that were significantly statistically different ($P \leq 0.05$) are indicated by * (vs. control) or # (CL+etomoxir vs. CL). See Methods section for details of statistical analyses.

concentrations of each compound (see figure legends) that gave significant (but less than maximal) inhibition of the parameters studied but with the retention of full cell viability.

Both the DGAT2 inhibitors tested (DGAT2-iC and DGAT2-iJ) resulted in a strong inhibition of the CL-stimulated

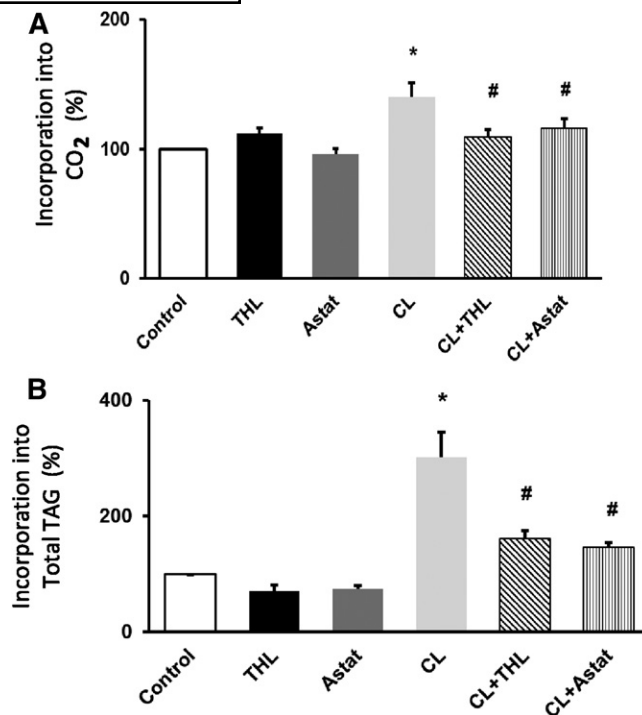


Fig. 4. ATGL inhibition prevents β₃-induced stimulation of U-¹⁴C-glucose incorporation into TAG and CO₂. Cells were incubated with CL for 2 h before addition of U-¹⁴C-glucose, and incorporation of label into (A) CO₂ and (B) TAG was measured during a further 2 h incubation (see Methods section). When Atglistatin (Astat) or THL were present, they were added at the same time as CL. Data are means (± SEM) for three separate experiments and are expressed with respect to control values that were set at 100% for each experiment. Values that were statistically significantly different ($P < 0.05$) are indicated by * (CL vs. control) and # (CL+THL or CL+Astat vs. CL).

incorporation of ¹⁴C-glucose into CO₂ and TAG-acyl groups (see Fig. 5A, B). By contrast, inhibition of DGAT1 (with DGAT1-iB) did not affect either incorporation of label into ¹⁴CO₂ (Fig. 5A) or into TAG-acyl groups (Fig. 5B). These observations suggest that DGAT2 activity is specialized for the esterification of de novo synthesized FAs into TAG and subsequent mitochondrial oxidation of FA products of TAG lipolysis. The validity of this conclusion is strengthened by the fact that the two inhibitors of DGAT2 used are structurally unrelated. Both DGAT1 and DGAT2 inhibition decreased significantly the glucose incorporation into the glyceride part of TAG (Fig. 5C), indicating that glycerol-3-P newly synthesized from glucose is incorporated into DG pools that are used by either DGAT1 or DGAT2 as substrates.

Importantly, the above observations were not altered qualitatively when experiments were conducted in the presence of added exogenous glycerol (0.75 mM) and oleate (0.75 mM in the presence of 0.25% albumin) to the medium (Fig. 5D–F); only DGAT2 inhibition resulted in the loss of labeling from U-¹⁴C-glucose into TAG-acyl moieties and CO₂ (Fig. 5D, E). Therefore, addition of exogenous oleate (or palmitate, not shown) did not affect the ability of DGAT2 inhibition specifically to affect the incorporation of de novo synthesized FA into TAG (compare

Plus oleate, glycerol

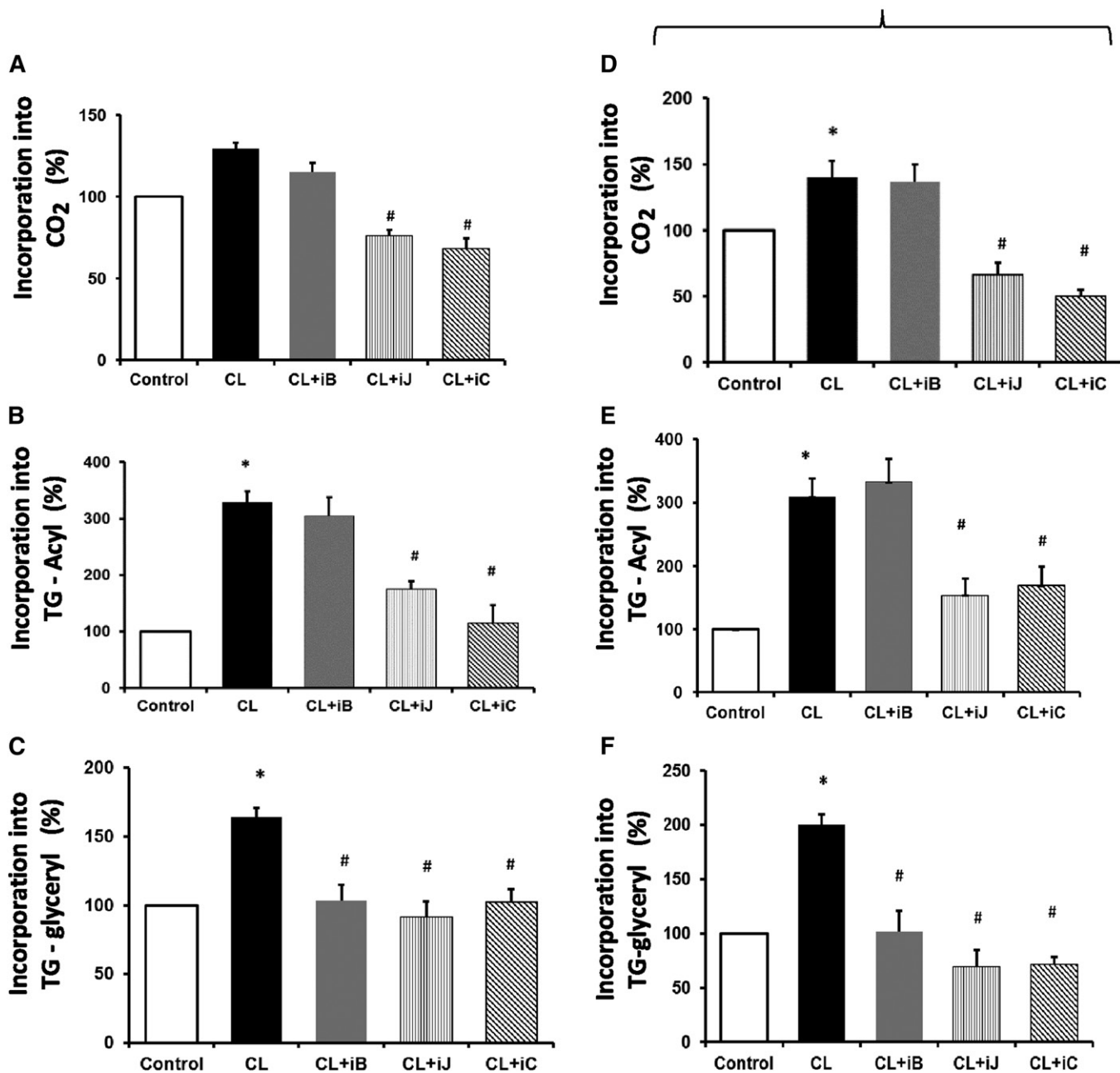


Fig. 5. Effect of DGAT1 and DGAT2 inhibition on the incorporation of U-¹⁴C glucose into CO₂ and TAG after β₃-agonist stimulation of IMBAT-1 cells. Cells were incubated with CL for 2 h before the start of incubations by the addition of U-¹⁴C-glucose label. Inhibitors were added individually 30 min before the addition of label (see Methods section). Experiments were performed in the absence (A–C) or presence (D–F) of oleate (0.75 mM with 0.25% BSA) and glycerol (0.75 mM). Incorporation of label from U-¹⁴C-glucose was measured for a 2 h period into CO₂ (A, D), TAG-acyl moieties (B, E), and TAG-glycerol moieties (C, F). The concentrations of inhibitors used were: DGAT1-iB, 0.75 μM; DGAT2-iC, 50 μM, and DGAT2-iJ, 50 μM. Values are means (± SEM) for three separate experiments and are expressed with respect to values for controls (set at 100%) to which no CL or inhibitors were added. Values that were statistically significantly different (*P* < 0.05) are indicated by * (CL vs. control) and # (CL + inhibitors vs. CL only).

Fig. 5B and 5E) or the formation of CO₂ after CL treatment. These observations indicate that de novo synthesized FA are compartmentalized rapidly into a pool of TAG which is not accessible to exogenously added FA. Addition of exogenous glycerol and oleate appeared to increase the effect of either DAGT1 or DGAT2 inhibition on glucose incorporation into TAG-glycerol, but did not affect the

relative importance of the two enzymes in this process (compare Fig. 5C and F).

DGAT1- AND DGAT2-KNOCKDOWN STUDIES. To exclude the possibility that nonspecific effects of enzyme inhibitors were compromising the validity of our observations, we investigated the longer-term effects of the knockdown of the expression of either protein using individually targeted

siRNA treatment of IMBAT-1 cells. The effects of 72 h siRNA treatment on mRNA expression of the DGAT1 and DGAT2 are shown in **Fig. 6**. A scrambled sequence was used in control cells. Note that reliable quantification of protein expression was not possible using a range of commercially available antibodies (not shown). Similarly, DGAT activities could not be reliably quantified by available DGAT assays using the amounts of material available. However, the fact that both inhibition and knockdown studies resulted in identical observations (see below) suggests that the large decreases in mRNA were accompanied by similar losses in enzyme activities and protein expression.

The data in **Fig. 7A** show that knockdown of DGAT2 had the same major inhibitory effect on the incorporation of label from U-¹⁴C-glucose into CO₂ both under basal and CL-stimulated conditions as shown by the inhibitors, confirming that de novo synthesized FA need to be incorporated into TAG by DGAT2 before they can undergo mitochondrial oxidation. Knockdown of DGAT1 had no effect at all (**Fig. 7A**). Therefore, these data are identical qualitatively

and quantitatively to those obtained using the respective DGAT1 and DGAT2 inhibitors (**Fig. 5**). Knockdown of DGAT2 also had a large inhibitory effect on the incorporation of glucose into total TAG (**Fig. 7B**). Saponification of the lipid fraction confirmed the preferential stimulus by CL of glucose incorporation into the acyl moieties of TAG, and showed that DGAT2 knockdown prevented the CL effects on the incorporation of label from U-¹⁴C-glucose into both TAG-acyl and TAG-glycerol moieties under both basal and CL-stimulated conditions (**Fig. 7E, F**). Therefore, effects of longer-term DGAT2 downregulation with siRNA treatment on the formation of TAG-acyl moieties and their subsequent use for ¹⁴CO₂ were identical to those observed after short-term inhibition (**Fig. 5**). By contrast, there was no effect on glucose incorporation onto TAG-acyl when DGAT1 was knocked down (**Fig. 7D**) and much smaller effects than those achieved by DGAT2 knockdown on incorporation of glucose into TAG-glycerol (**Fig. 7C**). These observations confirm that DGAT2 is specialized for the channelling of de novo synthesized fatty acids toward oxidation (to CO₂) initially through their incorporation into a distinct pool of TAG, followed by lipolysis (**Fig. 7C, E**).

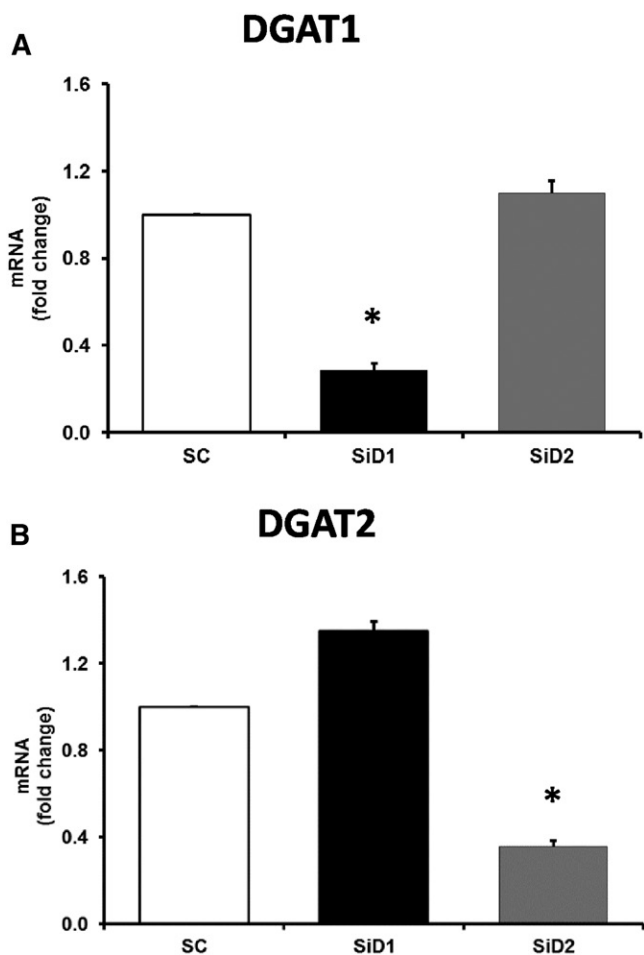


Fig. 6. Effects of siRNA-mediated DGAT1- or DGAT2-knockdown on the respective levels of mRNA expression of the two enzymes. Differentiated cells were treated for 72 h with either control (scrambled, SC) siRNA, or siRNA targeted toward DGAT1 (SiD1) or DGAT2 (SiD2) and the level of (A) DGAT1 and (B) DGAT2 mRNA expression was measured. Values (n = 3) are means (± SEM) for a representative experiment. Values that were statistically significantly different ($P < 0.05$) from SC are indicated by an asterisk.

DGAT2 knockdown attenuates the CL-mediated induction of UCP1 mRNA expression. In view of the observed close association between DGAT2 downregulation and metabolism of de novo synthesized FAs, we investigated whether long-term downregulation of DGAT2 or DGAT1 is accompanied by changes of lipogenic gene expression. We measured the mRNA expression (before and after CL treatment) of UCP1 and of several genes that are involved in the pathways leading from glucose to TAG synthesis and CO₂ formation (**Fig. 8**). Incubation of the cells with CL for 2 h increased the expression of UCP1 5-fold in IMBAT-1 cells [as observed previously in BAT in vivo (42)]; DGAT2 knockdown resulted in the halving of this increase whereas DGAT1 knockdown had no effect (**Fig. 8**). GPAT4 mRNA expression after CL treatment was decreased specifically by DGAT2 knockdown. None of the other genes tested (including Elvol3, not shown) showed significant differences in mRNA expression levels after CL-stimulation or knockdown of either DGAT compared with control (scrambled) siRNA-treated cells.

Therefore, knockdown of DGAT2 moderately but specifically affected the expression of genes that are central to elongation of de novo synthesized FA, FA esterification (GPAT4), and uncoupling of mitochondrial FA oxidation (UCP1) (3, 43, 44) indicating that it may play a central role in the maintenance of BAT function.

Direct oxidation of exogenously added oleate is very low. We next compared the roles of DGAT1 and DGAT2 in determining the metabolism of exogenously added, preformed fatty acids. We performed a series of experiments in which the normal concentration of unlabeled glucose was accompanied by glycerol (0.75 mM) and oleate (0.75 mM in the presence of 0.25% albumin). We performed parallel experiments in which we labeled either the glycerol (2-³H-glycerol) or oleate (1-¹⁴C-oleate). We also used U-¹⁴C-palmitate

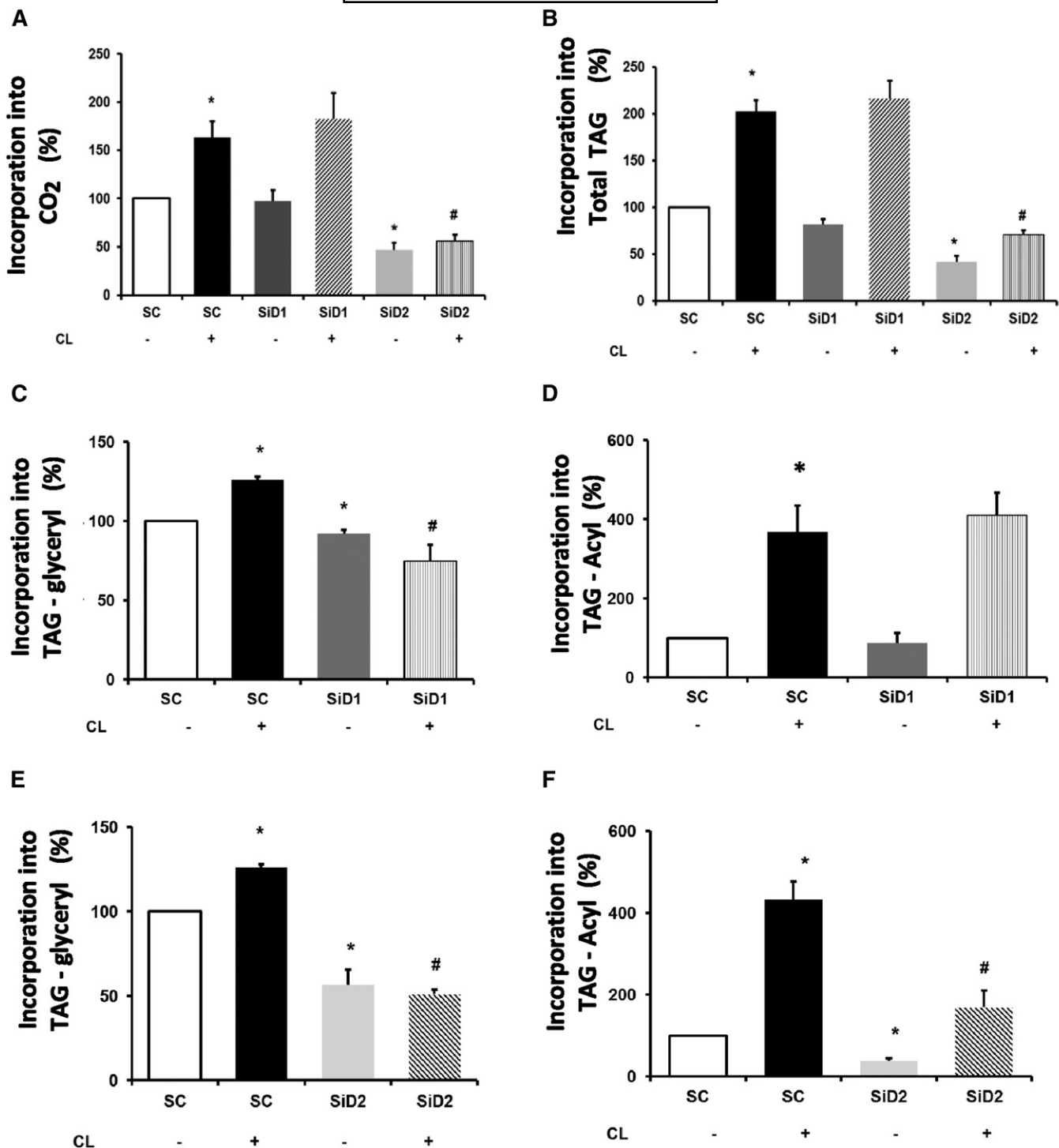


Fig. 7. Effects of siRNA-mediated DGAT1- or DGAT2-knockdown on the rates of incorporation of U-¹⁴C-glucose into CO₂ and TAG in the presence or absence of β₃-adrenergic stimulation of IMBAT-1 cells. Differentiated cells were treated for 72 h with either control (scrambled, SC) siRNA or siRNA (SiD) targeted toward DGAT1 (SiD1) or DGAT2 (SiD2) (see Methods section). Cells were incubated +/- CL for 2 h followed by the measurement of the incorporation of label from U-¹⁴C-glucose into (A) CO₂, (B) total TAG, and (C, E) TAG-glycerol and (D, F) TAG-acyl moieties of TAG. Data are means (± SEM) for three separate experiments and are expressed with respect to Control values (which are set at 100%) for each experiment. Values that are statistically significantly different (*P* < 0.05) are indicated by * (SC+CL or SiD vs. SC) and # (SiD+CL vs. SC+CL).

to verify that the effects observed with oleate could be replicated using a saturated FA; the results with palmitate (not shown) were identical to those obtained with oleate.

Contrary to the incorporation of de novo synthesized FA and glycerol-3-P derived from U-¹⁴C-glucose, the labeling

of TAG from either exogenous glycerol or oleate were not stimulated by CL, showing that the effects of the β₃-agonist were specific to the stimulation of glucose metabolism and FA derived from it. Although exogenous 1-¹⁴C-oleate was very rapidly incorporated into TAG (75 ± 9 nmol

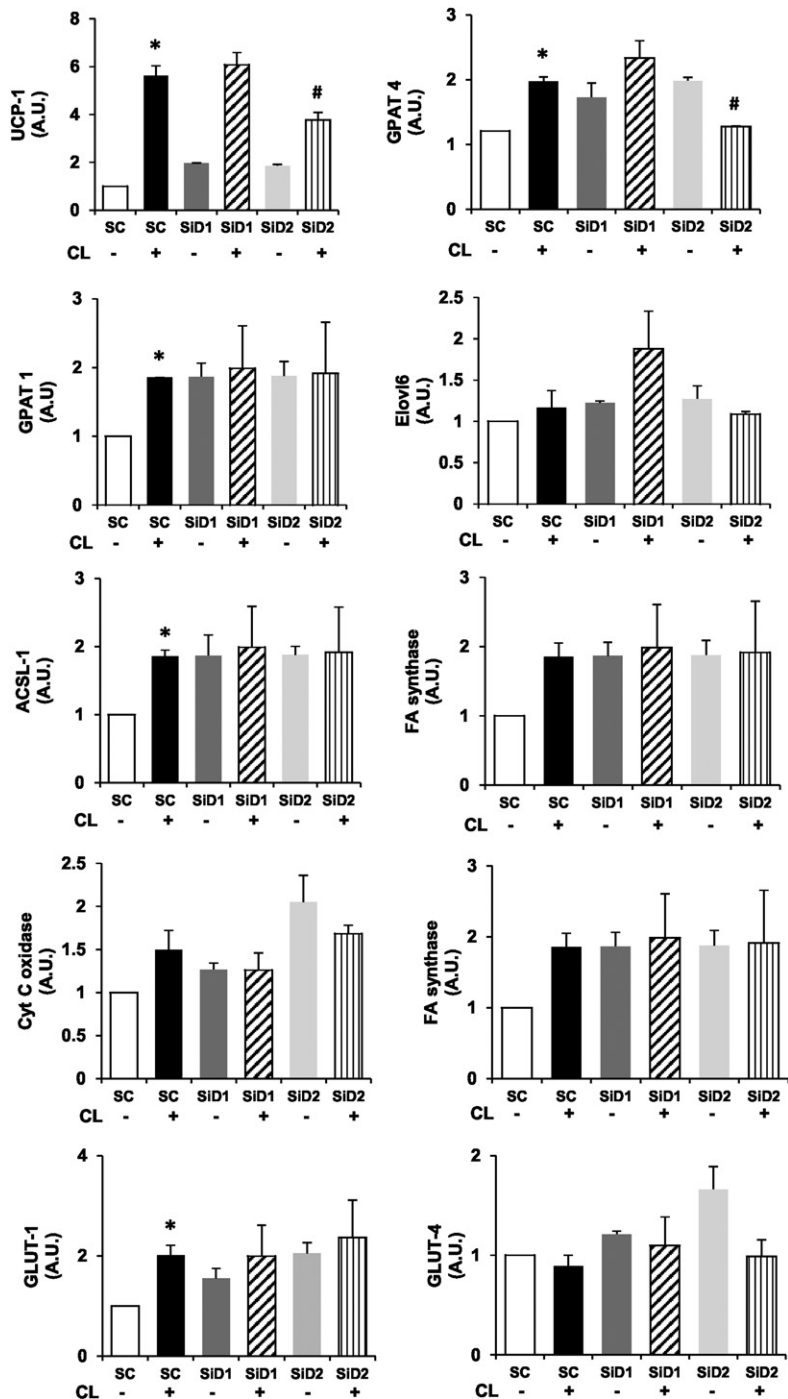


Fig. 8. Effect of siRNA-mediated knockdown of DGAT1 and DGAT2 on the expression of genes involved in pathways leading from glucose to TAG-synthesis and CO₂ formation. Differentiated cells were treated for 72 h with control siRNA (scrambled, SC) or siRNA targeted against DGAT1 (SiD1) or DGAT2 (SiD2). mRNA determinations were performed on cells incubated for 2 h either in the absence (-) or presence (+) of CL. The variances of input cDNA were normalized against the levels of three housekeeping genes: L19, B-actin, and 36B4, and expressed relative to those of SC, which were set at 1.0. Values are means (± SEM) for three separate experiments. Values that were statistically significantly different (*P* < 0.05) are indicated by * (vs. SC) and # (vs. SC+CL). ACC1, acetyl-CoA carboxylase 1; FASN, fatty acid synthase.

oleate/h/10⁶ cells), no significant ¹⁴C-label above background was recovered in oxidation products (either CO₂ or acid-soluble metabolites (ASMs)). Thus, although incubation with 1-¹⁴C-oleate (and U-¹⁴C-palmitate) achieved the same degree of overall cellular TAG labeling as that achieved by U-¹⁴C-glucose, only minimal ¹⁴C-label was recovered in CO₂ or ASMs after exposure to 1-¹⁴C-oleate even when incubations were extended to 8 h after addition of label to eliminate the possibility of a time-lag (not shown). There are two conclusions from these observations. First, that exogenous FAs are not oxidized directly to CO₂ to any significant extent, although they are rapidly incorporated into TAG. Second, that the pool of TAG into which

exogenous oleate is esterified is distinct from that into which glucose-derived de novo synthesized FAs are esterified by DGAT2, since the latter do give rise to ¹⁴CO₂ linearly over a 2 h incubation period. This is consistent with the observation in the “Oxidation of de novo synthesised FA is DGAT2-dependent” section above, that addition of exogenous oleate did not alter the pattern of fluxes of U-[¹⁴C]glucose into TAG-acyl or TAG-glycerol moieties. The simplest explanation for these combined observations is that exogenous (preformed) oleate is incorporated into a separate, large pool of TAG in which the specific activity of 1-¹⁴C-oleate is highly diluted, resulting in negligible labeling of the CO₂ produced from the oxidation of its constituent FA after

lipolysis. De novo synthesized fatty acids appear to have been incorporated into a TAG pool in which a much higher specific activity of the acyl groups was achieved. Therefore, this pool must be considerably smaller and must turn over rapidly to give the linear and immediate CO₂ formation observed.

These inferences were supported by the effects on exogenous 1-¹⁴C-oleate incorporation into TAG after the inhibition of either DGAT1 (using DGAT1-iB) or DGAT2 (using DGAT2-iJ). When added individually, each inhibitor affected only marginally the incorporation of exogenous 1-¹⁴C-oleate into TAG. However, incubation of cells simultaneously with both DGAT1-iB and DGAT2-iJ resulted in complete inhibition of labeling of TAG from exogenously added 1-¹⁴C-oleate (Fig. 9A). Therefore, the esterification of FAs derived from exogenous, preformed oleate (or palmitate, not shown) can be catalyzed redundantly by either DGAT1 or DGAT2. Only the combined inhibition of the two enzymes significantly decreased esterification of exogenously added oleate into TAG (Fig. 9A). This was entirely different from the ability of DGAT2 downregulation specifically to inhibit TAG-acyl labeling from glucose.

Incorporation of 2-[³H]glycerol into TAG was maximally decreased by inhibition of DGAT1 (Fig. 9B). Although DGAT2 inhibition also moderately decreased 2-³H-glycerol incorporation into TAG, this effect was much smaller than that of DGAT1 inhibition, and combined DGAT2 and DGAT1 inhibition did not increase that achieved by DGAT1 inhibition alone. Therefore, exogenous glycerol is used for the synthesis of DG, which serves preferentially as a substrate for DGAT1 (Fig. 9B), whereas glucose-derived glycerol-3-P is used preferentially for the synthesis of DG used by DGAT2 (Fig. 7E).

Experiments using mouse primary brown adipocytes

Having established the experimental conditions for the use of DGAT1 and DGAT2 inhibitors, we wanted to validate the salient aspects of our observations using mouse primary brown adipocytes. This enabled us to ascertain that the same conclusions are applicable in a cell system closer to the physiological condition.

CL stimulates etomoxir-sensitive glucose incorporation into CO₂. When primary brown adipocytes were treated with CL, the rate of CO₂ formation from U-¹⁴C-glucose was increased by 5.5-fold (Fig. 10A). This was prevented by etomoxir, indicating that the glucose had to be converted into FA before it was oxidized. This inference was confirmed by the demonstration that incubation with 5-(tetradecyloxy)-2-furoic acid (TOFA), an inhibitor of lipogenesis at the ATP-citrate lyase step, also inhibited the etomoxir-sensitive incorporation of glucose into CO₂ to the same extent (Fig. 10A). Although this scale of activation was similar to the 4-fold stimulation by CL of etomoxir-sensitive conversion of glucose into CO₂ observed in IMBAT-1 cells (see above), it occurred from a much lower background (control) of CO₂ production in control primary cells. The absolute rates of incorporation of U-¹⁴C-glucose into CO₂, TAG-acyl, and TAG-glycerol were 15.1 ± 1.1, 10.0 ± 1.5, and 10.0 ± 2.1 nmol/h/10⁶ cells, respectively. Therefore, primary brown

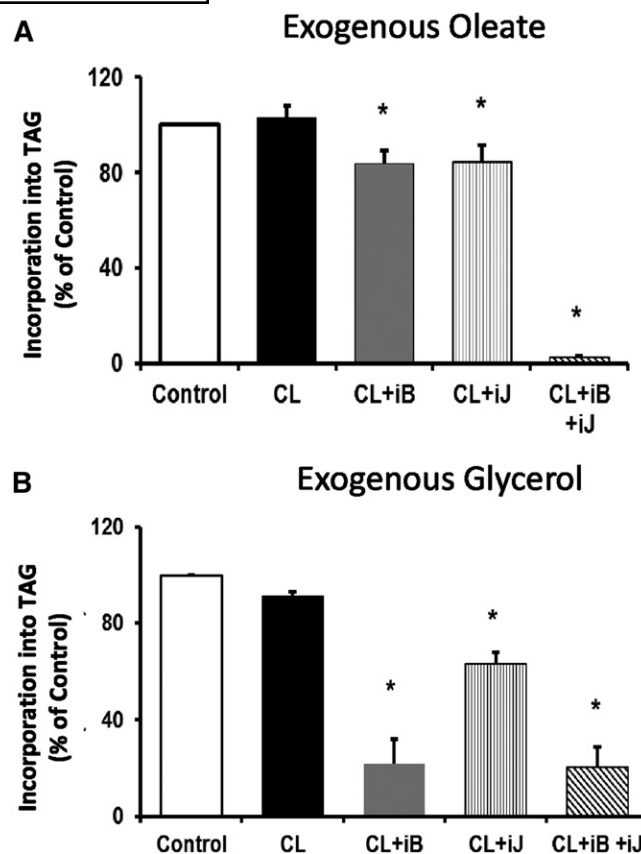


Fig. 9. Effects of individual or combined inhibition of DGAT1 and DGAT2 on the incorporation of added oleate or glycerol into TAG. Cells were incubated with glucose, oleate, and glycerol (see text for concentrations). When present, CL was added 2 h before the addition of label, either (A) 1-¹⁴C-oleate or (B) 2-³H-glycerol. The inhibitors (DGAT1-iB to inhibit DGAT1 and DGAT2-iJ to inhibit DGAT2, specifically) were added 30 min before the addition of label. Values are means (± SEM) for three separate experiments. Values that are statistically significantly different from those for control ($P < 0.05$) are indicated by an asterisk.

adipocytes had very similar rates of glucose incorporation as IMBAT-1 cells (see above) but were more oxidative, suggesting that the mobilization of the DGAT2-dependent TAG pool is even more rapid in primary cells.

Inhibition of DGAT2, but not DGAT1, prevents glucose conversion into CO₂. The CL-induced increase in CO₂ production from glucose was entirely prevented by inhibition of DGAT2 (Fig. 10A), confirming that, as in IMBAT-1 cells, the FA synthesized from glucose had to be incorporated into TAG before they could be oxidized (subsequent to lipolysis). By contrast, inhibition of DGAT1 had no effect on the etomoxir-sensitive conversion of glucose into CO₂. Therefore, the data obtained with primary brown adipocytes fully confirmed the evidence for a specialized role of DGAT2 in channelling de novo synthesized FAs toward oxidation in brown adipocytes. The effect of DGAT2 was mimicked by inhibition of CPT1 with etomoxir and by the inhibition of de novo lipogenesis by TOFA (Fig. 10A) confirming that DGAT2 action lies on a pathway linking DNL to FA oxidation in brown adipocytes.

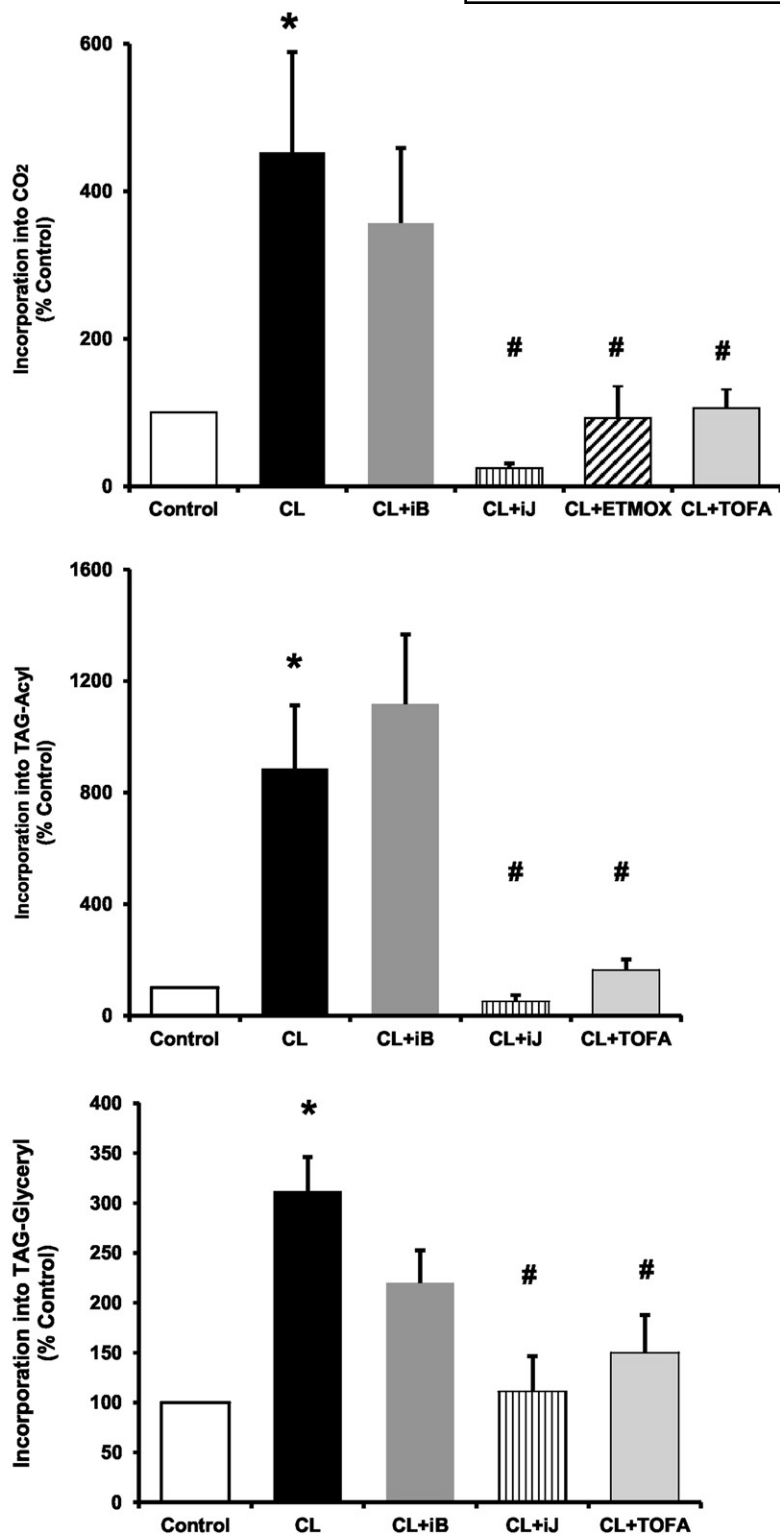


Fig. 10. Effect of DGAT1 and DGAT2 inhibition on the incorporation of U-¹⁴C glucose into CO₂ and TAG after β3-agonist stimulation of primary brown adipocytes. Cells were incubated with CL for 2 h before the start of incubations by the addition of U-¹⁴C-glucose label. Inhibitors were added individually 30 min before the addition of label (see Methods section). Experiments were performed in the presence of oleate (0.75 mM with 0.25% BSA) and glycerol (0.75 mM). Incorporation of label from U-¹⁴C-glucose was measured for a 2 h period into (A) CO₂, (B) TAG-acyl, and (C) TAG-glycerol moieties. The concentrations of inhibitors used were: DGAT1-iB, 0.75 μM; DGAT2-iC, 50 μM, and DGAT2-iJ, 50 μM. Values are means (± SEM) for three separate experiments and are expressed with respect to values for controls (set at 100%) to which no CL or inhibitors were added. Values that were statistically significantly different ($P < 0.05$) are indicated by * (CL vs. Control) and # (CL + inhibitors vs. CL only). See Methods section for details of statistical analysis. Etmox, etomoxir.

Inhibition of DGAT2 but not of DAGT1 prevents incorporation of U-¹⁴C-glucose into TAG. Glucose incorporation into TAG-acyl and TAG-glycerol moieties were both prevented by DGAT2 inhibition in primary brown adipocytes (Fig. 10 B, C). Moreover, this effect was mimicked by the inhibition of de novo FA synthesis with TOFA (an inhibitor of de novo lipogenesis) indicating that DGAT2 utilizes newly synthesized diglycerides and FA to

form a distinct pool of TAG. Inhibition of DGAT1 had no effect at all on incorporation of labeled glucose into TAG-acyl groups (as observed in IMBAT-1 cells). Although there was a tendency for the inhibition of DGAT1 to affect incorporation into TAG-glycerol groups, the effect was less than that shown by DGAT2 inhibition (as in IMBAT-1 cells), and did not reach statistical significance (Fig. 10 C).

DISCUSSION

Glucose is one of the two major substrates used by BAT. The high rate of glucose uptake during cold exposure acts as a 'glucose sink', and has been suggested to be able to improve insulin sensitivity physiologically during cold exposure (9, 45) and potentially to form the basis for pharmacological strategies aimed at increasing glucose utilization by BAT to regulate blood glucose in obesity and diabetes (12, 45, 46). However, BAT bioenergetics are centered around the uncoupled oxidation of FAs as the source of thermogenic capacity. Glucose-derived pyruvate makes only a minor direct contribution toward mitochondrial electron transport chain activity, although there is a strong relationship between FA oxidation and glucose uptake in BAT (47). The simultaneous activation of glucose transport, de novo fatty acid synthesis and fatty acid oxidation in brown adipocytes by β -adrenergic stimulation (14, 48, 49) is consistent with the observations of increased expression of enzymes involved in FA synthesis (e.g., FSN), FA desaturation (SCD1) and FA elongation (e.g., Elvol3, Elvol6) after cold-exposure or CL-treatment in vivo (13, 23, 37). However, the rationale for the oxidation of newly synthesized FAs has previously been questioned and considered paradoxical (9, 10). It has been proposed that the newly synthesized FAs are not oxidized immediately but are stored in lipid droplets in anticipation of subsequent thermogenic activation (10, 24, 30).

The present study has addressed this apparent paradox by showing that, in brown adipocytes (primary cells and IMBAT-1 cell line), glucose-derived FAs are specifically channelled into a rapidly mobilized pool of TAG, which is distinct from the bulk TAG pool into which exogenous, preformed FAs are esterified. This is evidenced by the DGAT2-dependence of the labeling of CO₂ derived from de novo synthesized FA, but not that derived from exogenous oleate, in spite of equivalent overall labeling of total cellular TAG by either substrate. The ability of TOFA (an inhibitor of FA synthesis) to replicate the effects of DGAT2 inhibition supports the concept that channelling of de novo synthesized FA toward oxidation occurs via DGAT2-mediated TAG synthesis. This segregation of a glucose-derived, DGAT2-dependent synthesis of a distinct pool of TAG enables the cell to oxidize de novo synthesized FA directly, and independently from preformed FA derived exogenously. Therefore, DGAT2 acts as the link between increased glucose utilization and uncoupled mitochondrial FA oxidation, as part of a concerted response of this pathway to adrenergic stimulation in brown adipocytes (see Fig. 11). Previous observations in vivo had found evidence for distinct pools of TAG being used to channel FAs toward oxidation or esterification (50, 51) and for the difference of the stereospecific distribution of de novo synthesized and exogenous FAs in cellular TAG (52, 53). The current observations on the specialized role of DGAT2 in brown adipocytes provide a mechanism through which these distinct TAG pools could be achieved, if the concept can be extended to other cell types.

When we tested this concept in primary brown adipocytes, we found that, in this cellular model too, DGAT2

(but not DGAT1) inhibition totally prevented incorporation of glucose into TAG-acyl and TAG-glycerol moieties, and the formation of CO₂ from de novo synthesized FAs. Indeed, because primary brown adipocytes are more oxidative than IMBAT-1 cells, the role of DGAT2 in mediating the channelling of glucose carbons toward FA oxidation was even more pronounced. Moreover, we demonstrated that the effect of DGAT2 inhibition on these parameters could be mimicked by inhibition of de novo lipogenesis with TOFA, thus confirming the close link between DGAT2 action and utilization of de novo synthesized FAs for TAG synthesis and subsequent oxidation.

The specialized role of DGAT2 in esterifying de novo synthesized FAs is similar to that described originally in HepG2 cells (1, 2). More recently, urokinase-type plasminogen activator has been shown to stimulate TAG synthesis from acetate, in parallel with increased DNL and the specific induction of the expression of DGAT2 (54). These observations suggest that this specialized function of DGAT2 may be a ubiquitous function of this enzyme in different cell types, with metabolic outcomes depending on tissue function; e.g., linking glycemia to triglyceridemia in the liver (2) and the channelling of glucose-derived FA toward rapid oxidation in BAT (present data).

The ability of ATGL inhibition to prevent the CL-mediated stimulation of CO₂ formation from de novo synthesized FA derived from glucose would be expected to result from the interruption of FA supply by inhibition of TAG lipolysis. However, in addition, ATGL inhibition also prevented the stimulation of glucose incorporation into TAG (both glyceride and acyl moieties) indicating that a product of lipolysis activates glucose metabolism by the cells through a positive feedback mechanism (Fig. 11). Inhibition of TAG lipolysis is suggested to have interrupted this feedback activation of one or more steps leading from glucose to the synthesis of glycerol-3-P, de novo FA synthesis, and esterification into TAG. This is consistent with previous observations that in *Atgl*^{-/-} mice, BAT shows diminished glucose uptake (55), and that ATGL expression is essential for β 3-activation of DNL in BAT in vivo (37, 55). Our data suggest that DNL is specifically stimulated to a greater extent than incorporation of glucose-derived glycerol moieties into TAG; therefore, positive feedback activation of DNL may occur partly independently of the stimulation of triose-phosphate formation. The importance of ATGL in the provision of ligands for the positive feedback-activation of PPAR α target gene activation is well established (56).

A proportion of the CO₂ labeling from U-¹⁴C-glucose arises during lipogenesis and the direct oxidation of the resulting acetyl-CoA through the TCA cycle; this is known to make only a minor contribution toward thermogenesis (19). We distinguished between this direct oxidation of glucose and the CO₂ derived from FA oxidation by using etomoxir. This inhibitor of CPT1 decreased CO₂ labeling only moderately in the absence of CL but totally prevented the stimulation (4-fold in IMBAT-1 cells and 5.5-fold in primary adipocytes) mediated by CL, indicating that the increased formation of ¹⁴CO₂ from glucose after CL stimulation was entirely due to increased oxidation of de novo

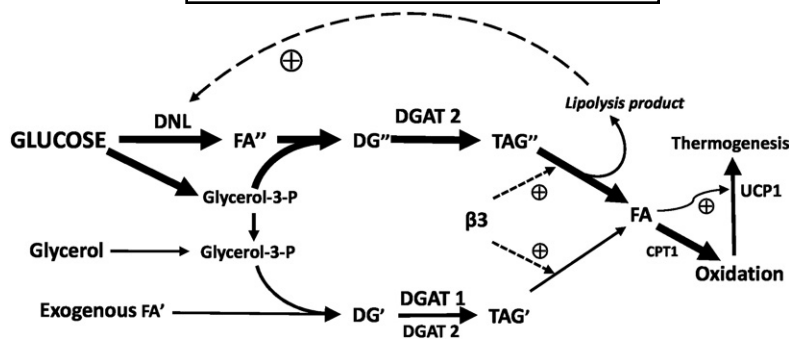


Fig. 11. Proposed pathways that link DGAT2 to de novo fatty acid synthesis and thermogenesis in brown adipocytes. Fatty acids synthesized de novo from glucose (FA'') are used to form a pool of diglyceride (DG'') which is esterified with FA'' by DGAT2 to form a distinct pool of triglyceride (TAG''). Adrenergic (β_3) stimulation simultaneously activates de novo lipogenesis and TAG lipolysis. A product of lipolysis activates the process of glucose utilization for lipogenesis (DNL) upon stimulation of the cells by β_3 -agonists through a positive feedback mechanism which is interrupted by inhibition of ATGL. TAG lipolysis provides FA substrate for uncoupled mitochondrial oxidation. FA activate UCP1, the expression of which is increased by β_3 -action. Glycerol-3-P synthesized from exogenous glycerol is used for the synthesis of a separate DG pool (DG') which is used as a substrate for re/esterification preferentially by DGAT1, and to a lesser extent by DGAT2. Glycerol-3-P generated endogenously from glucose is used to form both DG'' and DG'. Exogenous FA is not oxidized directly, but is re/esterified by DGAT1 or DGAT2 redundantly into/within a larger TAG pool (TAG') before oxidation.

synthesized FAs. Importantly, the CL-mediated and etomoxir-sensitive stimulation of CO_2 labeling from glucose was specifically prevented by downregulation of DGAT2 but not of DGAT1. This indicated that *i*) DNL and TAG synthesis precede the formation of CO_2 , and *ii*) that DGAT2 is specifically involved in this pathway. Such sensitivity to DGAT2 downregulation reinforces the conclusion that CO_2 production does not occur directly from the de novo synthesized FAs but only subsequent to TAG formation. Oxidation of exogenously added fatty acids is deduced to have been similarly indirect in IMBAT-1 cells because detection of labeled CO_2 or ASM formation was very low when cells were incubated with $1\text{-}^{14}\text{C}$ -oleate or $U\text{-}^{14}\text{C}$ -palmitate, in spite of their very rapid labeling of cellular TAG. This was also the case in primary cells (not shown). This can be explained if the added ^{14}C -oleate was esterified into a large, preexisting pool of TAG within which its specific activity was highly diluted. This indirect route for FA oxidation has been described for several tissues and cell types (57–60).

It is well-established that the activation of ATGL by β_3 -adrenergic agonism promotes TAG turnover by simultaneously promoting glucose uptake and DNL, including the induction of proteins involved in DNL (37), thus providing substrates for DGAT2. Because of the importance of long-chain acyl-CoA synthase 1 (ACSL1) in channelling FA (whether supplied exogenously or synthesized de novo) toward mitochondrial β -oxidation and of GPAT4 in diverting FA toward TAG synthesis (27, 61), we considered whether the very low rates of labeling of $^{14}\text{CO}_2$ from exogenously added $1\text{-}^{14}\text{C}$ -oleate to generate directly could have been due to a low expression of ACSL1 from IMBAT-1 cells. This possibility was excluded because we detected high levels of expression of ACSL1 mRNA (Fig. 8). In addition, adequate expression of ACSL1 can also be inferred from the observation that de novo synthesized FAs were oxidized rapidly to CO_2 simultaneously with TAG labeling from glucose in a

DGAT2-dependent manner. GPAT4 expression was at least partly dependent on continued DGAT2 expression in IMBAT-1 cells (Fig. 8B), and may play a major role in ensuring that both endogenously derived and exogenously added FAs are esterified to TAG prior to oxidation.

In IMBAT-1 cells, DGAT1 and DGAT2 act redundantly for the incorporation of glucose-derived glycerol-3-P into TAG, although less so after longer-term knockdown. However, exogenous glycerol is used preferentially for the formation of DG utilized by DGAT1, indicating that the two enzymes also have differential access to DG synthesized from exogenous or endogenously synthesized glycerol-3-P. This compartmentalization is different from the observations previously made on two liver systems [HepG2 cells (1) and murine liver (5)] in which DGAT2 is specialized for the incorporation of exogenous glycerol into TAG. This difference in the handling of glycerol-3-P formed from exogenous glycerol may reflect the differences between the metabolism of TAG in liver and BAT. Thus, lipolysis in BAT goes to completion (to glycerol and FA) whereas it is mostly restricted to the formation of DG and monoglyceride in the liver; e.g., in rat liver in vivo (62, 63) and in primary rat hepatocytes (64). Therefore, in BAT, the lipolysis-reesterification cycling occurs between TAG and FA whereas in the liver, cycling occurs primarily between DG and TAG, or monoglyceride and DG (64) without the release of glycerol. In the liver, DG is mostly used for the resynthesis of TAG either for maintenance of cytosolic TAG stores in lipid droplets or incorporated into VLDL (1, 2, 65). The specialization of specific enzyme isoforms for the channelling of FA is increasingly being recognized [see (61, 66)].

In summary, all our data on primary brown adipocytes and a brown adipocyte-derived cell line indicate that the DGAT2-dependent pool of TAG is distinct from that into which exogenous, preformed FAs are esterified. As a result, newly synthesized FAs are made immediately available for mitochondrial oxidation in a DGAT2-dependent manner.

By contrast, exogenous FAs are esterified into a separate, larger, preexisting pool of TAG. Assuming that this pool of TAG is itself mobilized during β -adrenergic stimulation, this indicates that exogenous FAs and de novo synthesized FAs are esterified into separate TAG pools before being oxidized. However, whereas DGAT2 is exclusively responsible for the formation of the TAG pool specific for de novo synthesized FAs, it also participates, together with DGAT1, in the (re)esterification of exogenous FAs into the larger pool of cellular TAG. These data suggest that within the multilocular structure of BAT lipid droplets, a sub-population of droplets originate specifically as a result of DGAT2 activity, enriched in de novo synthesized FAs and preferentially mobilized to enable glucose to contribute immediately toward thermogenesis. This is consistent with the previous observation that within a given cell, individual lipid droplets have differential access to the TAG biosynthetic machinery (67).

The very high level of expression of DGAT2 mRNA in the tissue in vivo and its large fold-induction and persistence during IMBAT-1 cell differentiation are indicative of the importance of DGAT2 expression for BAT function. In this context, the 4-fold induction of UCPI1 in IMBAT-1 cells upon CL-stimulation is markedly blunted after knockdown of DGAT2 expression, suggesting that DGAT2 expression is important for the maintenance of the brown adipocyte phenotype. It is noteworthy that *Dgat2*^{-/-} mice do not survive beyond 12 h after birth. This has been ascribed to defects in skin lipid synthesis and the associated dehydration (7). Our data raise the possibility that they may also be unable to thermoregulate normally. It is well established that deficient thermogenesis results in increased mortality in neonatal rodents (68) and that prevention of glucose uptake by BAT in vivo by downregulation of mTORC2 results in hypothermia (16). Although it is likely that the contribution that glucose makes toward heat production in BAT is not fully developed in the neonate [owing to the lower rates of DNL in the tissue before weaning (14)] it would become more important as the pups switch to a high carbohydrate diet upon weaning (at 3 weeks of age) such that glucose- and DGAT2-dependent nonshivering thermogenesis might become critical for survival postweaning. 

The authors thank Jensen (Johnson & Johnson) and AstraZeneca for the provision of inhibitor compounds.

REFERENCES

1. Wurie, H. R., L. Buckett, and V. A. Zammit. 2012. Diacylglycerol acyltransferase 2 acts upstream of diacylglycerol acyltransferase 1 and utilizes nascent diglycerides and de novo synthesized fatty acids in HepG2 cells. *FEBS J.* **279**: 3033–3047.
2. Zammit, V. 2013. Hepatic triglyceride synthesis and secretion: DGAT2 as the link between glycaemia and triglyceridaemia. *Biochem. J.* **451**: 1–12.
3. Wendel, A. A., D. Cooper, O. R. Ilkayeva, D. Muoio, and R. A. Coleman. 2013. Glycerol-3-phosphate acyltransferase (GPAT)-1, but not GPAT4, incorporates newly synthesized fatty acids into triacylglycerol and diminishes fatty acid oxidation. *J. Biol. Chem.* **288**: 27299–27306.
4. Eichmann, T. O., M. Kumari, J. Haas, R. V. Farese, Jr., R. Zimmermann, A. Lass, and R. Zechner. 2012. Studies on the substrate and stereo/regioselectivity of adipose triglyceride lipase, hormone-sensitive lipase, and diacylglycerol-O-acyltransferases. *J. Biol. Chem.* **287**: 41446–41457.
5. Qi, J., W. Lang, J. G. Geisler, P. Wang, I. Petrounia, S. Mai, C. Smith, H. Askari, G. T. Struble, R. Williams, et al. 2012. The use of stable isotope-labeled glycerol and oleic acid to differentiate the hepatic functions of DGAT1 and -2. *J. Lipid Res.* **53**: 1106–1116.
6. Chen, H. C., S. J. Smith, Z. Ladha, D. R. Jensen, L. D. Ferreira, L. K. Pulawa, J. G. McGuire, R. E. Pitas, R. H. Eckel, and R. V. Farese. 2002. Increased insulin and leptin sensitivity in mice lacking acyl-CoA:diacylglycerol acyltransferase 1. *J. Clin. Invest.* **109**: 1049–1055.
7. Stone, S., H. M. Myers, S. M. Watkins, B. E. Brown, K. R. Feingold, P. M. Elias, and R. V. Farese. 2004. Lipopenia and skin barrier abnormalities in DGAT2-deficient mice. *J. Biol. Chem.* **279**: 11767–11776.
8. Li, C., L. Li, J. Lian, R. Watts, R. Nelson, B. Goodwin, and R. Lehner. 2015. Roles of acyl-CoA:diacylglycerol acyltransferases 1 and 2 in triacylglycerol synthesis and secretion in primary hepatocytes. *Arterioscler. Thromb. Vasc. Biol.* **35**: 1080–1091.
9. Townsend, K. L., and Y. H. Tseng. 2014. Brown fat fuel utilization and thermogenesis. *Trends Endocrinol. Metab.* **25**: 168–177.
10. Cannon, B., and J. Nedergaard. 2004. Brown adipose tissue: function and physiological significance. *Physiol. Rev.* **84**: 277–359.
11. Villarroya, F., and A. Vidal-Puig. 2013. Beyond the sympathetic tone: the new brown fat activators. *Cell Metab.* **17**: 638–643.
12. Whittle, A. J., M. Lopez, and A. Vidal-Puig. 2011. Using brown adipose tissue to treat obesity - the central issue. *Trends Mol. Med.* **17**: 405–411.
13. Hankir, M. K., M. A. Cowley, and W. K. Fenske. 2016. A BAT-centric approach to the treatment of diabetes: turn on the brain. *Cell Metab.* **24**: 31–40.
14. Trayhurn, P. 1981. Fatty acid synthesis in mouse brown adipose tissue. The influence of environmental temperature on the proportion of whole-body fatty acid synthesis in brown adipose tissue and the liver. *Biochim. Biophys. Acta.* **664**: 549–560.
15. Olsen, J. M., M. Sato, O. S. Dallner, A. L. Sandstrom, D. F. Pisani, J. C. Chambard, E. Z. Amri, D. S. Hutchinson, and T. Bengtsson. 2014. Glucose uptake in brown fat cells is dependent on mTOR complex 2-promoted GLUT1 translocation. *J. Cell Biol.* **207**: 365–374.
16. Albert, V., K. Svensson, M. Shimobayashi, M. Colombi, S. Munoz, V. Jimenez, C. Handschin, F. Bosch, and M. N. Hall. 2016. mTORC2 sustains thermogenesis via Akt-induced glucose uptake and glycolysis in brown adipose tissue. *EMBO Mol. Med.* **8**: 232–246.
17. Saggerson, E. D., T. W. McAllister, and H. S. Baht. 1988. Lipogenesis in rat brown adipocytes. Effects of insulin and noradrenaline, contributions from glucose and lactate as precursors and comparisons with white adipocytes. *Biochem. J.* **251**: 701–709.
18. Ma, S. W., and D. O. Foster. 1986. Uptake of glucose and release of fatty acids and glycerol by rat brown adipose tissue in vivo. *Can. J. Physiol. Pharmacol.* **64**: 609–614.
19. Brito, M. N., N. A. Brito, S. R. Brito, M. A. Moura, N. H. Kawashita, I. C. Kettelhut, and R. Migliorini. 1999. Brown adipose tissue triacylglycerol synthesis in rats adapted to a high-protein, carbohydrate-free diet. *Am. J. Physiol.* **276**: R1003–R1009.
20. Cooney, G. J., and E. A. Newsholme. 1982. The maximum capacity of glycolysis in brown adipose tissue and its relationship to control of the blood glucose concentration. *FEBS Lett.* **148**: 198–200.
21. Minokoshi, Y., M. Saito, and T. Shimazu. 1988. Sympathetic activation of lipid synthesis in brown adipose tissue in the rat. *J. Physiol.* **398**: 361–370.
22. Yu, X. X., D. A. Lewin, W. Forrest, and S. Adams. 2002. Cold elicits the simultaneous induction of fatty acid synthesis and beta-oxidation in murine brown adipose tissue: prediction from differential gene expression and confirmation in vivo. *FASEB J.* **16**: 155–168.
23. Tan, C. Y., S. Virtue, G. Bidault, M. Dale, R. Hagen, J. L. Griffin, and A. Vidal-Puig. 2015. Brown adipose tissue thermogenic capacity is regulated by Elovl6. *Cell Reports.* **13**: 2039–2047.
24. Festuccia, W. T., P. G. Blanchard, V. Turcotte, M. Laplante, M. Sariahmetoglu, D. N. Brindley, D. Richard, and Y. Deshaies. 2009. The PPARgamma agonist rosiglitazone enhances rat brown adipose tissue lipogenesis from glucose without altering glucose uptake. *Am. J. Physiol. Regul. Integr. Comp. Physiol.* **296**: R1327–R1335.
25. Orava, J., P. Nuutila, M. E. Lidell, V. Oikonen, T. Noponen, T. Viljanen, M. Scheinin, M. Taittonen, T. Niemi, S. Enerback, et al. 2011. Different metabolic responses of human brown adipose tissue to activation by cold and insulin. *Cell Metab.* **14**: 272–279.
26. Isler, D., H. P. Hill, and M. Meier. 1987. Glucose metabolism in isolated brown adipocytes under beta-adrenergic stimulation. Quantitative contribution of glucose to total thermogenesis. *Biochem. J.* **245**: 789–793.

27. Ellis, J. M., L. O. Li, P. C. Wu, T. R. Koves, O. Ilkayeva, R. D. Stevens, S. Watkins, D. M. Muoio, and R. Coleman. 2010. Adipose acyl-CoA synthetase-1 directs fatty acids toward beta-oxidation and is required for cold thermogenesis. *Cell Metab.* **12**: 53–64.
28. Moura, M. A., W. T. Festuccia, N. H. Kawashita, M. A. Garofalo, S. R. Brito, I. C. Kettelhut, and R. Migliorini. 2005. Brown adipose tissue glyceroneogenesis is activated in rats exposed to cold. *Pflugers Arch.* **449**: 463–469.
29. Wu, C., C. Orozco, J. Boyer, M. Leglise, J. Goodale, S. Batalov, C. L. Hodge, J. Haase, J. Janes, J. W. Huss 3rd, et al. 2009. BioGPS: an extensible and customizable portal for querying and organizing gene annotation resources. *Genome Biol.* **10**: R130.
30. Labbe, S. M., A. Caron, I. Bakan, M. Laplante, A. C. Carpentier, R. Lecomte, and D. Richard. 2015. In vivo measurement of energy substrate contribution to cold-induced brown adipose tissue thermogenesis. *FASEB J.* **29**: 2046–2058.
31. Rosell, M., M. Kaforou, A. Frontini, A. Okolo, Y. W. Chan, E. Nikolopoulou, S. Millership, M. E. Fenech, D. MacIntyre, J. O. Turner, et al. 2014. Brown and white adipose tissues: intrinsic differences in gene expression and response to cold exposure in mice. *Am. J. Physiol. Endocrinol. Metab.* **306**: E945–E964.
32. Hulver, M. W., J. R. Berggren, R. N. Cortright, R. W. Dudek, R. P. Thompson, W. J. Pories, K. G. MacDonald, G. W. Cline, G. I. Shulman, G. L. Dohm, et al. 2003. Skeletal muscle lipid metabolism with obesity. *Am. J. Physiol. Endocrinol. Metab.* **284**: E741–E747.
33. Wurie, H. R., L. Buckett, and V. A. Zammit. 2011. Evidence that diacylglycerol acyltransferase 1 (DGAT1) has dual membrane topology in the endoplasmic reticulum of HepG2 cells. *J. Biol. Chem.* **286**: 36238–36247.
34. Saggerson, E. D., and A. L. Greenbaum. 1970. The regulation of triglyceride synthesis and fatty acid synthesis in rat epididymal adipose tissue. *Biochem. J.* **119**: 193–219.
35. Payne, V. A., W. S. Au, S. L. Gray, E. D. Nora, S. M. Rahman, R. Sanders, R. Hadaschik, J. E. Friedman, S. O'Rahilly, and J. J. Rochford. 2007. Sequential regulation of diacylglycerol acyltransferase 2 expression by CAAT/enhancer-binding protein beta (C/EBPbeta) and C/EBPalpha during adipogenesis. *J. Biol. Chem.* **282**: 21005–21014.
36. Zammit, V. A. 1999. The malonyl-CoA-long-chain acyl-CoA axis in the maintenance of mammalian cell function. *Biochem. J.* **343**: 505–515.
37. Mottillo, E. P., P. Balasubramanian, Y. H. Lee, C. Weng, E. E. Kershaw, E. E., and J. Granneman. 2014. Coupling of lipolysis and de novo lipogenesis in brown, beige, and white adipose tissues during chronic beta3-adrenergic receptor activation. *J. Lipid Res.* **55**: 2276–2286.
38. Haemmerle, G., T. Moustafa, G. Woelkart, S. Buttner, A. Schmidt, T. van de Weijer, M. Hesselink, D. Jaeger, P. C. Kienesberger, K. Zierler, et al. 2011. ATGL-mediated fat catabolism regulates cardiac mitochondrial function via PPAR-alpha and PGC-1. *Nat. Med.* **17**: 1076–1085.
39. Tang, T., M. J. Abbott, M. Ahmadian, A. B. Lopes, Y. Wang, and H. Sul. 2013. Desnutrin/ATGL activates PPARdelta to promote mitochondrial function for insulin secretion in islet beta cells. *Cell Metab.* **18**: 883–895.
40. Camus, G., E. Herker, A. A. Modi, J. T. Haas, H. R. Ramage, R. V. Farese, Jr., and M. Ott. 2013. Diacylglycerol acyltransferase-1 localizes hepatitis C virus NS5A protein to lipid droplets and enhances NS5A interaction with the viral capsid core. *J. Biol. Chem.* **288**: 9915–9923.
41. Herker, E., C. Harris, C. Hernandez, A. Carpentier, K. Kaehlecke, A. R. Rosenberg, R. V. Farese, R. V. Jr, and M. Ott. 2010. Efficient hepatitis C virus particle formation requires diacylglycerol acyltransferase-1. *Nat. Med.* **16**: 1295–1298.
42. Mottillo, E. P., A. E. Bloch, T. Leff, and J. Granneman. 2012. Lipolytic products activate peroxisome proliferator-activated receptor (PPAR) alpha and delta in brown adipocytes to match fatty acid oxidation with supply. *J. Biol. Chem.* **287**: 25038–25048.
43. Nagel, C. A., L. Vergnes, H. Dejong, S. Wang, T. M. Lewin, K. Reue, and R. A. Coleman. 2008. Identification of a novel sn-glycerol-3-phosphate acyltransferase isoform, GPAT4, as the enzyme deficient in *Agpat6*^{-/-} mice. *J. Lipid Res.* **49**: 823–831.
44. Yamashita, A., Y. Hayashi, N. Matsumoto, Y. Nemoto-Sasaki, S. Oka, T. Tanikawa, and T. Sugiura. 2014. Glycerophosphate/Acylglycerophosphate acyltransferases. *Biology (Basel)*. **3**: 801–830.
45. Stanford, K. L., R. J. Middelbeek, K. L. Townsend, D. An, E. B. Nygaard, K. M. Hitchcox, K. R. Markan, K. Nakano, M. F. Hirshman, Y. H. Tseng, et al. 2013. Brown adipose tissue regulates glucose homeostasis and insulin sensitivity. *J. Clin. Invest.* **123**: 215–223.
46. Bartelt, A., O. T. Bruns, R. Reimer, H. Hohenberg, H. Itrich, K. Peldschus, M. G. Kaul, U. I. Tromsdorf, H. Weller, C. Waurisch, et al. 2011. Brown adipose tissue activity controls triglyceride clearance. *Nat. Med.* **17**: 200–205.
47. Marette, A., and L. Bukowiecki. 1991. Noradrenaline stimulates glucose transport in rat brown adipocytes by activating thermogenesis. Evidence that fatty acid activation of mitochondrial respiration enhances glucose transport. *Biochem. J.* **277**: 119–124.
48. Yu, Y. H., Y. Zhang, P. Oelkers, S. L. Sturley, D. J. Rader, and H. Ginsberg. 2002. Posttranscriptional control of the expression and function of diacylglycerol acyltransferase-1 in mouse adipocytes. *J. Biol. Chem.* **277**: 50876–50884.
49. Knight, B. L., A. Hebbachi, D. Hauton, A. M. Brown, D. Wiggins, D. D. Patel, and G. F. Gibbons. 2005. A role for PPARalpha in the control of SREBP activity and lipid synthesis in the liver. *Biochem. J.* **389**: 413–421.
50. Banke, N. H., A. R. Wende, T. C. Leone, J. M. O'Donnell, E. D. Abel, D. P. Kelly, and E. Lewandowski. 2010. Preferential oxidation of triacylglyceride-derived fatty acids in heart is augmented by the nuclear receptor PPARalpha. *Circ. Res.* **107**: 233–241.
51. Bu, S. Y., and D. G. Mashek. 2010. Hepatic long-chain acyl-CoA synthetase 5 mediates fatty acid channeling between anabolic and catabolic pathways. *J. Lipid Res.* **51**: 3270–3280.
52. Henderson, R. J., W. W. Christie, and J. H. Moore. 1979. Positional distribution of exogenous and endogenous fatty acids in triacylglycerols formed by rat adipocytes in vitro. *Biochim. Biophys. Acta.* **574**: 8–17.
53. Henderson, R. J., W. W. Christie, and J. H. Moore. 1979. Esterification of exogenous and endogenous fatty acids by rat adipocytes in vitro. *Biochim. Biophys. Acta.* **573**: 12–22.
54. Paland, N., A. Gamliel-Lazarovich, R. Coleman, and B. Fuhrman. 2014. Urokinase-type plasminogen activator (uPA) stimulates triglyceride synthesis in Huh7 hepatoma cells via p38-dependent up-regulation of DGAT2. *Atherosclerosis.* **237**: 200–207.
55. Hoy, A. J., C. R. Bruce, S. M. Turpin, A. J. Morris, M. A. Febbraio, and M. Watt. 2011. Adipose triglyceride lipase-null mice are resistant to high-fat diet-induced insulin resistance despite reduced energy expenditure and ectopic lipid accumulation. *Endocrinology.* **152**: 48–58.
56. Ahmadian, M., M. J. Abbott, T. Tang, C. S. Hudak, Y. Kim, M. Bruss, M. K. Hellerstein, H. Y. Lee, V. T. Samuel, G. I. Shulman, et al. 2011. Desnutrin/ATGL is regulated by AMPK and is required for a brown adipose phenotype. *Cell Metab.* **13**: 739–748.
57. Badin, P. M., D. Langin, and C. Moro, C. 2013. Dynamics of skeletal muscle lipid pools. *Trends Endocrinol. Metab.* **24**: 607–615.
58. Guo, Z., B. Burguera, and M. Jensen. 2000. Kinetics of intramuscular triglyceride fatty acids in exercising humans. *J. Appl. Physiol.* **89**: 2057–2064.
59. Kanaley, J. A., S. Shadid, M. T. Sheehan, Z. Guo, and M. Jensen. 2009. Relationship between plasma free fatty acid, intramyocellular triglycerides and long-chain acylcarnitines in resting humans. *J. Physiol.* **587**: 5939–5950.
60. Kanaley, J. A., S. Shadid, M. T. Sheehan, Z. Guo, and M. Jensen. 2013. Hyperinsulinemia and skeletal muscle fatty acid trafficking. *Am. J. Physiol. Endocrinol. Metab.* **305**: E540–E548.
61. Cooper, D. E., T. Grevengoed, E. L. Klett, and R. A. Coleman. 2015. Glycerol-3-phosphate Acyltransferase Isoform-4 (GPAT4) Limits Oxidation of Exogenous Fatty Acids in Brown Adipocytes. *J. Biol. Chem.* **290**: 15112–15120.
62. Yang, L. Y., A. Kuksis, J. J. Myher, and G. Steiner. 1995. Origin of triacylglycerol moiety of plasma very low density lipoproteins in the rat: structural studies. *J. Lipid Res.* **36**: 125–136.
63. Yang, L. Y., A. Kuksis, J. J. Myher, and G. Steiner. 1996. Contribution of de novo fatty acid synthesis to very low density lipoprotein triacylglycerols: evidence from mass isotopomer distribution analysis of fatty acids synthesized from [2H6]ethanol. *J. Lipid Res.* **37**: 262–274.
64. Lankester, D., A. Brown, and V. Zammit. 1998. Use of cytosolic triacylglycerol hydrolysis products and of exogenous fatty acid for the synthesis of triacylglycerol secreted by cultured hepatocytes. *J. Lipid Res.* **39**: 1889–1895.
65. Zammit, V. A., L. K. Buckett, A. V. Turnbull, H. Wurie, and A. Proven. 2008. Diacylglycerol acyltransferases: Potential roles as pharmacological targets. *Pharmacol. Ther.* **118**: 295–302.
66. Ong, K. T., M. T. Mashek, S. Y. Bu, A. S. Greenberg, and D. G. Mashek. 2011. Adipose triglyceride lipase is a major hepatic lipase that regulates triacylglycerol turnover and fatty acid signaling and partitioning. *Hepatology.* **53**: 116–126.
67. Kuerschner, L., C. Moessinger, and C. Thiele. 2008. Imaging of lipid biosynthesis: how a neutral lipid enters lipid droplets. *Traffic.* **9**: 338–352.
68. Adams, B. A., S. L. Gray, E. R. Isaac, A. C. Bianco, A. J. Vidal-Puig, and N. Sherwood. 2008. Feeding and metabolism in mice lacking pituitary adenylate cyclase-activating polypeptide. *Endocrinology.* **149**: 1571–1580.